博士論文

Ph.D Dissertation

Superposition states in quantum optics: teleportation experiments, modeling theory, tomography algorithms

（非古典状態の量子テレポーテーション実験の研究─
条件付き操作、理論モデル、トモグラフィアルゴリズム）

2012年02月

東京大学大学院　　　工学系研究科　　　物理工学専攻

The University of Tokyo　　School of Engineering　　Departement of Applied Physics

ベニキ　ユーゴ
Benichi　　Hugo

Superposition states in quantum optics: teleportation experiments, modeling theory, tomography algorithms

（非古典状態の量子テレポーテーション実験の研究―条件付き操作、理論モデル、トモグラフィアルゴリズム）

Hugo Benichi

Acknowledgments

The work presented in this manuscript was carried out at the Applied Physics department of the University of Tokyo, in the laboratory of Prof. Akira Furusawa. Starting from April 2009 and over the three years of doctor course I have spend at the Applied Physics department, I could start and complete my research project in a very fruitful research environment and in almost ideal working conditions. I am very grateful to the laboratory and to my supervisor for this wonderful research environment I had the chance to experience and be privileged with. I also would like to thank all the people of the laboratory, student, staff, and especially co-experimentalists, for their infinite help and support in many occasions, be it about research, daily life in Japan or administrative tasks.

Being a foreigner in Japan certainly has its challenges. Overall, moving from France to Japan I feel I had the chance to receive a very warm and hearty welcome and could integrate myself smoothly and find my place in this wonderful country, thanks to the help from the people of my laboratory, the great support from the staff of the University of Tokyo, and the international student community here. Especially, I would like to thank all my friends at the University of Tokyo, those who have already graduated and those who will still be studying after me, for interesting discussions about life in Japan, for cheering me up, for listening to my incessant rambling, and overall many good moments and memories. I am also very grateful to Japan and the Ministry of Education for giving me the financial support and opportunity to study three years at the University of Tokyo and obtain the doctoral degree in such favorable conditions.

I cannot close this section without looking back on the long road which brought me here as I think that getting the Ph.D title eventually plays out in more than three years. First and foremost, it is my family I want to thank, to whom I owe my education and personal values, my curiosity and taste for understanding my surroundings. I also thank my home country which gave me the rare opportunity to study at such wonderful schools and learn from so many knowledgeable and wise teachers and professors who gave me the willingness to succeed and pursue in scientific studies as far as I did until today. In that regard, my greatest thanks go especially to the professoral staff of the Physics department at Ecole Polytechnique and Ecole Normale Supérieure.

Contents

List of Figures

List of Symbols

Symbol	Description
Variables and parameters	
x, q	position variable
p	momentum variable
$\alpha = (x + ip)/\sqrt{2}$	complex amplitude
t	time
ω, Ω	angular frequency and sideband angular frequency
s	squeezing power
r	EPR correlation power
η	loss coefficient
Operators	
$\hat{x}, \hat{p}$	position and momentum operators
$\hat{a}, \hat{a}^\dagger$	annihilation and creation operators
$\hat{\rho}$	density matrix
$\hat{D}(\alpha), \hat{D}_\alpha$	displacement operator
$\hat{S}(s), \hat{S}_s$	squeezing operator
$\hat{U}(\theta), \hat{U}_\theta$	phase-shifter operator
$\hat{B}(\theta), \hat{B}_\theta$	beam-splitter operation
Phase-space quasi-distributions	
$W(q,p), W_{q,p}, W(\alpha)$	Wigner function
$Q(q,p), Q_{q,p}, Q(\alpha)$	Hushimi function
$P(q,p), P_{q,p}, P(\alpha)$	Glauber-P function
$\chi(u,v), \chi_{u,v}, \chi(\xi)$	Characteristic function
$\mathcal{R}, \mathcal{R}^{-1}$	Radon and inverse Radon transforms
Polynomial series and special functions	
$H_n(x)$	Hermite polynomials
$T_n(x), U_n(x)$	Chebysheff's polynomials, first and second kind
$Z_s^n(r,\phi) = R_s^n(r)e^{in\phi}$	complex Zernike polynomials
$J_n(r)$	Bessel's functions of the first kind
$\mathrm{erf}(x)$	error function
Mathematical operations	
$\circ, \star$	1-dimensional convolution
$\circ\circ, \star\star$	2-dimensional convolution
$\mathrm{tr}()$	trace operation
$\otimes$	tensor product

Table 1: Recurrent mathematical symbols and notations.

Introduction

The field of Quantum Optics

Quantum optics could be defined as the study of the quantum properties of propagating waves of the electrical field. In other words, quantum optics is the description of light waves at the quantum level using quantum mechanics. Historically, the modern theory of quantum optics has been developed by Roy J. Glauber[47] in the sixties with his work on quantum coherence initiated to explain the Hanbury Brown-Twiss interferometer experiment and the photon bunching phenomena [7]. It was already known before that time that a quantum description of the electrical field was necessary to grasp the understanding of certain phenomena involving interaction between light and matter. Although the idea of the existence of particles of light appeared several times in the historical development of physics, the precise idea of quanta of light dates back to the beginning of the nineteenth century and to Plank[1] and Einstein's work[2]. As a matter of fact, the word "photon" itself was first proposed by Einstein to put a name on the concept of quanta of light. These ideas were later experimentally verified by Arthur Compton[4]. Despite these early development which also turned out to be the root of quantum mechanics itself and one of its first experimental hints, the modern theory of quantum optics was rather late to emerge. Before Glauber simplified the complex formalism of quantum field theory into a simpler theoretical framework for quantum optics, quantitative studies were only possible using the complete theory of quantum electrodynamics and radiation. Nowadays, we have gained a very good understanding of the quantum description of light, a question which for the most part is solved as far as fundamental sciences go.

Nevertheless quantum optics is nowadays a very active field of research. As it turns out, the electrical field is the most simple physical system for fundamental tests of quantum physics. The superposition principle, quantum entanglement, Bose-Einstein statistics, interferences; all essential properties of quantum mechanics can be observed and studied in quantum optics easily all the better thanks to the absence of direct photon-photon interactions. Experimental quantum optics was essentially started with the access to coherent light sources and Theodore H. Maiman's first ruby laser [9]. From the first pioneering laser systems of the sixties to current state-of-the-art experiments, xperimental quantum optics has advanced steadily and passed several important milestones. In the sixties, seventies and eighties, the development of more powerful laser systems at new wavelengths allowed for the study of non-linear optics[10]. In the eighties, progress progress in the study and understanding of parametric-down conversion and four wave mixing phenomena led to the observationand demonstration of squeezed light and "two-photons coherent states", as squeezing was called at that time[15, 16, 17]. The availability of squeezed quantum states eventually paved the road to many quantum optics experiments, starting with the first Gaussian information processing experiments[29] and qubit experiments[23] of the late nineties. In the last ten years experimental quantum optics has been the testing ground of further experiments and fundamental tests of quantum mechanics, focusing on the generation, measurement, characterisation and manipulation of exotic or entangled quantum states of light. Inspired by the "gedenken experiment" of the founding fathers of quantum mechanics, these exotic quantum states of light

such as the elusive Schroedinger's cat state are now routinely produced in laboratories[41, 40, 51].

The rapid development of quantum optics was possible thanks to the rather unlikely combination of four ingredients: 1) lasers which produce very pure coherent light of all frequencies are now a mainstream technology, easy to produce, deploy and operate. 2) in the particular optical region of the electromagnetic spectrum, background light is virtually void of any black body radiations, so that a clean and quiet environment down to the level of the quantum vacuum can be easily obtained in the laboratory. 3) with electronics noise levels far below the optical shotnoise level, high energy conversion efficiency and linearity, silicon PIN photodiodes allow for easy measurements of the quantum state of light down to the quantum vacuum level. 4) easy passive manipulation of light through the index of refraction gives us a complete toolbox of so-called linear optical components which forms the backbone of most experimental setups: optical lenses, dielectric and Bragg mirrors, amplitude modulators, birefringent materials, waveguides.

Quantum Information Processing

Quantum mechanics calls for a different treatment of information processing than what Claude E. Shannon achieved with his classical theory of information[6]. With the swift development of computer technologies following the end of World War II and the invention of the transistor, it quickly appeared to physicists that quantum mechanics could certainly have a special status in information processing[12, 14]. Although the question is still open in computational complexity theory and although the exact relation between complexity classes associated with quantum computers like BQP (bounded error quantum polynomial time) and QMA (quantum analog of the deterministic complexity class NP or the probabilistic complexity class MA) and classical complexity classes is still unknown, it is firmly believed that quantum computers can genuinely solve a number of computational problems faster than classical computers . Some famous quantum algorithms like Shor's factoring algorithm[27] or Grover's search algorithm[25] are hints of this conjecture and of the advantage of quantum computers.

From the original idea of a quantum analogical computer by Feynman[12] and the experimental proof of violation of the Bell's inequalities[11] and therefore the genuine existence of quantum entanglement, the field of quantum information processing is now a major sub-field of quantum mechanics. Quantum information processing has now also become the major and most active research topic in the field of quantum optics. Of course, quantum information processing can be studied with several different physical systems, but light provides an especially adequate medium for the implementation of quantum communication and information algorithms, thanks to the absence of direct photon-photon interactions and the tendency of photons to stay undisturbed. In that respect, light waves have some genuine advantages for the practical applications and realization of quantum entanglement, quantum measurement and complex quantum information phenomena.

As a striking example of quantum communication protocols, teleportation was discovered early on in the development of the field of quantum information processing. With either qubit [21] and continuous variable flavors [22], experiments were soon to follow [23, 29]. Until now continuous variable teleportation has only been performed with the class of so-called Gaussian states [29, 52, 58, 64]. However, this alone is not sufficient for universal quantum computation where non-Gaussianity of some kind has been shown to be necessary: at least third order nonlinear operations are necessary for building a universal quantum computer[30], something Gaussian operations and Gaussian states alone cannot achieve. For instance photon-subtraction techniques which are based on discrete variable and qubit technology, can provide these useful non-linearities and are used to generate Schroedinger's cat states and other optical non-Gaussian states[24]. Schroedinger's cat states are of particular interest as they have been shown to be a useful resource for fault-tolerant QIP[56]. Although such non-Gaussian non-classical states of light that would allow for such uni-

versal operations have been available experimentally for some time in the continuous variable regime [41, 40, 51], the major challenge of actually manipulating these states in some Gaussian protocol context beyond simple generation has remained mostly unaddressed. Therefore, it appears crucial to extend the well understood Gaussian continuous variable technology and linear optics with non-Gaussian states and non-Gaussian operations.

Subject of the thesis

The main subject of this thesis is the experimental study of the quantum teleportation process with as input states non-Gaussian quantum states of light approximating small amplitude Schroedinger's cat states. More precisely, we are interested in the experimental demonstration of the quantum teleportation of non-classical states of light up to the point where the output quantum state are still without ambiguity non-classical quantum states. This experiment is ambitious for it lies on top of two different frontiers of experimental quantum optics. On the one side we inherit from the long lineage of continuous variable Gaussian experiments and have built a quantum teleportation apparatus which transcends the sideband regime. On the other side we have used the photon subtraction protocol to generate in the laboratory these highly non-classical non-Gaussian states necessary for universal quantum information processing. In this thesis manuscript we report on how we have combined these two sets of technologies and how we could demonstrate successful Gaussian manipulation of non-classical non-Gaussian states by achieving experimental quantum teleportation of Schroedinger's cat states of light. Using the photon-subtraction protocol we generate quantum states approximating closely Schroedinger's cat states in a manner similar to [41, 40, 51]. To accommodate with the required time-resolving photon detection techniques and handle the wave-packet nature of these optical Schroedinger's cat states, we have developed a hybrid teleporter built with continuous-wave light yet able to directly operate in the time domain. For this purpose we have constructed a time-gated source of EPR correlations as well as a zero phase-dispersion classical channel. We were able to bring all the experimental parameters up to the quantum regime and performed successful quantum teleportation in the sense that both our input and output states are strongly non-classical quantum states of light. As a prototype of these new techniques in a fully quantum regime, this experiment constitutes a first step towards more advanced QIP protocols and future non-classical state manipulation experiments in quantum optics.

This thesis manuscript explains in details and reports on the results of the experiment discribed above, but also includes several related theoretical studies and analysis linked to this experimental work. Overall, these theoretical studies can be divided in three groups. First, there is the question of understanding precisely what we observe in the teleportation experiment. This requires a complete phase space model of input state, teleportation process, and output teleported state, taking into account in addition the relevant experimental parameters. The second point, which is to some extent related to the first, is to correctly understand the multimode properties of the input photon subtracted state and of the broadband teleporter apparatus to model the transient and time-domain nature of this experiment. The third point is about studies on the process of quantum tomography, which is a necessity for current state-of-the-art experiments in continuous variable quantum optics for characterization of unknown quantum states.

Content of the manuscript

The main content of this thesis manuscript is divided into four chapters. Additional material mostly related to experimental details can be found in the appendix sections.

- The first chapter is a summary and succinct presentation of the theory of quantum optics. It

mostly focuses on the physics of a single quantum harmonic oscillator, which is reviewed in the Heisenberg picture, Schroedinger picture, and phase space formalism. It also introduces models for the main experimental measurement techniques available in quantum optics used in this thesis.

- The second chapter focuses exclusively on the single photon subtraction protocol, the tool of choice nowadays to generate small amplitude Schroedinger's cat states of light and other low photon number non-Gaussian states. It presents our experimental setup and results as well as a detailed analysis and quantum theoretical model for this family of photon subtracted states so important for the field of quantum information processing.

- The third chapter deals with the problem of quantum tomography and its practical numerical implementation. The core of the chapter is a demonstration and further study of one of the main results of this thesis, an algorithm for the reconstruction of the Wigner function using polynomial series decomposition and stable linear inversion. It is followed by a detailed analysis of the statistical error in tomography reconstruction algorithms, illustrated with Monte-Carlo simulations.

- The fourth and last chapter presents the main experimental results of this thesis: the experimental deterministic and conditional teleportation of Schroedinger's cat states of light. It includes a simple presentation of the elementary theory of teleportation, and an extended model of wave-packet teleportation. In addition, it gives a description of the experimental setup, presents experimental results and their analysis using the model mentioned above.

The reading order proposed by this manuscript chapters arrangement does not have to be strictly observed, as chapters **??**, **??** and **??** are mostly independent, to the exception of experimental results of Chaps.**??** and **??**. Chapter 1 is included in this manuscript mostly as a necessary reference for the good understanding of equations and mathematical derivations and the rigorous definition of operators and mathematical objects appearing in the following chapters. However, some paragraphs in chapter 1, most notably in Secs.1.3 and 1.5 go beyond simple textbook material and are referenced at several latter points.

Academic Publications and Conferences

The results of this thesis have been published in several scientific journal publications. In chronological order, they are:

- N. Lee, H. Benichi, Y. Takeno, S. Takeda, J. Webbs, E. Hungtington, and A. Furusawa, "Quantum teleportation of nonclassical wave packets: An effective multimode theory", *Science* **332**, 330 (2011).

- H. Benichi, S. Takeda, N. Lee, and A. Furusawa, "Teleportation of Non-Classical Wave-Packets of light", *Phys. Rev. A* **84**, 012308 (2011).

- H. Benichi, and A. Furusawa, "Optical homodyne tomography with polynomial series expansion", *Phys. Rev. A* **84**, 032104 (2011).

The first of this article presents the main experimental results on Schroedinger's cat state teleportation, which is the subject of Chap.**??** for teleportation, and Chap.**??** for Schroedinger's cat state generation. The second article presents a detailed theoretical model of the experiment, with careful considerations of its broadband characteristics. This model can be found in Chap.**??**, over Secs.**??** and **??**. The last article presents a related work on quantum tomography and demonstrate a new

reconstruction algorithm of the Wigner function, which is included in Chap.**??**. At the time of writing, another article reporting on the results of Gaussian conditional teleportation is in preparation. The work of this thesis has also been presented through posters and presentations at the following international and domestic conferences:

- ButsuriGakkai64, 64th fall meeting of the Japanese Society of Physics, Kumamoto University, Japan, Sep 2009 (presentation, 25pZF-2).

- QIT21, the 21st Quantum Information Technology Symposium, Tokyo, Japan, Nov 2009 (presentation).

- SPQT 2010, Quantum Measurement and Control workshop, Sydney, Australia, Feb 2010 (poster).

- ISPQT 2010, International symposium on Physics of Quantum Technology, Tokyo, Japan, Apr 2010 (poster, 8TH-01).

- QCMC 2010, Tenth International Conference on Quantum Communication, Measurement and Computation, Brisbane, Australia, Jul 2010 (poster, P3-10).

- FIRST 2010, Annual meeting of the FIRST project on quantum information processing, Atami, Japan, Dec 2010 (poster).

- CLEO 2011, Conference on Laser and Electro-Optics, Baltimore USA, May 2011 (presentation, JTuF4).

Finally, during the CLEO US 2011 conference, the work of this thesis has been awarded by the Optical Society of America (OSA) with the Theodore Maiman Outstanding Student Prize, first prize, including a $3000 cash prize.

Chapter 1

Quantum Theory of Light

In this first chapter, we expose the basic theory of quantum optics and give to the reader all the necessary elements to understand the content of the subsequent chapters. In Sec.1.1, we present the postulates of quantum mechanics which are assumed and used through the thesis. In Sec.1.2, we introduce the standard textbook toolbox of monomode quantum optics. In Sec.1.3, we focus on the phase-space representation of quantum states of light which constitutes our representation of choice for the analysis of experimental results in Chaps.**??**, **??** and **??**. In Sec.1.4, we extend our monomode toolbox with the more uncommon formulae of multimode quantum optics. Finally in Sec.1.5, we presents basic elements on the thoery of the detection of light and measurements in quantum optics as well as useful models for non-ideal imperfect detection devices.

1.1 Quantum mechanics postulates

The main axioms of quantum mechanics are by themselves already quite rich of consequences on the physics of quantum phenomena and quantum systems. Therefore, before looking at the specific details of quantum optics, it is important to precisely define these axioms. We start first with some basic elements on general quantum mechanics.

1.1.1 Hilbert space representation

Usually, the first postulate of quantum mechanics is the *postulate of description* which assumes the existence of a complete $\mathbb{C}$-vector space usually labeled $\mathcal{H}$ and whose norm-unity vectors are assumed to be the possible *quantum states* of a given physical system. To any *pure* physical state corresponds a unity norm vector in $\mathcal{H}$, and any unity norm vector in $\mathcal{H}$ describes a possible physical state of the syste and carries all information about it. Here, *pure* is a sementic term we will explain in Sec.1.1.4. This vector space $\mathcal{H}$ is commonly called the *Hilbert space* of the system. $\mathcal{H}$ can be finite or infinite dimensional. An element of $\mathcal{H}$ is a vector which is usually written with the *ket* convention $|x\rangle \in \mathcal{H}$ introduced by Dirac. Linear forms on $\mathcal{H}$ are written with the *bra* convention $\langle x| : \mathcal{H} \to \mathbb{C}$. The *bra* / *ket* notation is useful to express the inner product, or scalar product, on $\mathcal{H}$

$$(|x\rangle, |y\rangle) = \langle y|x\rangle \in \mathbb{C}, \tag{1.1.1}$$

which is also called a *bra-ket*. $\mathcal{H}$ is a vector space and guarantees the validity of the *superposition principle*: quantum states written as sums of the form $|\psi\rangle \propto (|\alpha\rangle - |\alpha'\rangle)$ are valid physical states of the system, provided their norm is unity. This principle is at the heart of many phenomena in quantum physics and is of interest to us as we will see in Chap.**??**. Furthermore, $\mathcal{H}$ is a complete space which guarantees the existence of infinitely many orthonormal basis. There can be countable

basis $\{|x_n\rangle\}_{n\in I}$ satisfying the scalar orthorgonality relation

$$\langle x_n|x_m\rangle = \delta_n^m, \tag{1.1.2}$$

and uncountable basis $\{|x\rangle\}_{x\in\Lambda}$ satisfying the similar fonctional orthorgonality relation

$$\langle x|x'\rangle = \delta(x - x'). \tag{1.1.3}$$

These two species of orthogonal basis are usually respectively called *discrete* and *continuous* basis in the context of quantum physics. Any quantum state $|\psi\rangle$ can be decomposed on $\{|x_n\rangle\}_{n\in I}$

$$|\psi\rangle = \sum_{n\in I} c_n|x_n\rangle, \text{ where } c_n = \langle x_n|\psi\rangle, \tag{1.1.4}$$

or on $\{|x\rangle\}_{n\in\Lambda}$

$$|\psi\rangle = \int_\Lambda dx c(x)|x\rangle, \text{ where } c(x) = \langle x|\psi\rangle, \tag{1.1.5}$$

Finally, $\mathcal{H}$ is a vector space on $\mathbb{C}$, which postulates the existence of a *quantum phase* and the associated quantum interference phenomena. The quantum phase is most of time dynamical in nature and can be calculated with the Schroedinger's equation. It can also carry interactions in quantum field SU1 gauge theories, or results from cyclic adiabtic trajectories in phase space in which case it is called *geometric phase*[3].

1.1.2 Operators

Linear operators on $\mathcal{H}$, written $\hat{O} : \mathcal{H} \to \mathcal{H}$, describe how external interactions or the self dynamic of the physical system change a quantum state $|x\rangle$ into $|y\rangle = \hat{O}|x\rangle$. The identity operator is written $\hat{\mathbb{1}}$. If it exists, the inverse of $\hat{U}$ is written $\hat{U}^{-1}$. $\hat{U}$ is unitary if and only if $\hat{U}\hat{U}^{-1} = \hat{U}^{-1}\hat{U} = \hat{\mathbb{1}}$. With the bra-ket notation, the projector on $|x\rangle$ is easily written $\hat{P}_{|x\rangle} = |x\rangle\langle x|$. Any orthonormal basis $\{|x_n\rangle\}_n$ follows the closure relation

$$\hat{\mathbb{1}} = \sum_n \hat{P}_{|x_n\rangle} = \sum_n |x_n\rangle\langle x_n|, \tag{1.1.6}$$

where the identity is decomposed onto a complete sum of orthogonal projectors cutting the Hilbert space in as many subvector spaces. In finite dimensional Hilbert spaces, any operator $\hat{A}$ can be expressed as a matrix in the orthonormal basis $\{|n\rangle\}$

$$\hat{A} = \sum_{n,m} A_{n,m}|n\rangle\langle m|, \text{ where } A_{n,m} = \langle n|\hat{A}|m\rangle. \tag{1.1.7}$$

This representation is still valid with discrete orthonormal basis in infinite-dimensional Hilbert spaces. The Hermitian adjoint of $\hat{A}$ is written $\hat{A}^\dagger$. If and only if $\hat{A} = \hat{A}^\dagger$, $\hat{A}$ is an Hermitian operator whose eigenvalues are real numbers. According to the spectral theorem, any Hermitian operator $\hat{A}$ can be diagonalized on the basis of its eigenvectors $\{|y_n\rangle\}$ as a sum of projectors

$$\hat{A} = \sum_n \langle y_n|\hat{A}|y_n\rangle \hat{P}_{|y_n\rangle} = \sum_n a_n|y_n\rangle\langle y_n|, \tag{1.1.8}$$

where $a_n = \langle y_n|\hat{A}|y_n\rangle$ are the real valued eigenvalues of $\hat{A}$.

1.1.3 Projective measurements

The second postulate of quantum mechanics is the *measurement postulate*. In its weak version, it states that any measurable variable or property of the system can be represented as a Hermitian operator $\hat{A} = \hat{A}^\dagger$ whose eigenvalues a_n are the only possible outcome of any experimental measurement of this variable. The probability p_n of measuring $a_n = \langle y_n | \hat{A} | y_n \rangle$ when the system is in the state $|\psi\rangle$ is assumed to be

$$p_n = |\langle y_n | \psi \rangle|^2. \tag{1.1.9}$$

After the measurement of a_n happening with probability p_n, the state of the system is projected with probability 1 onto the corresponding eigenstate $|y_n\rangle$. The expectation value $\langle a \rangle$ of the variable represented by $\hat{A}$ is therefore by definition

$$\langle a \rangle = \sum_n p_n a_n. \tag{1.1.10}$$

With Eq.(1.1.8), $\langle a \rangle$ is also

$$\langle a \rangle == \langle \psi | \hat{A} | \psi \rangle. \tag{1.1.11}$$

The variance Δa^2 of the measurement is simply $\langle a^2 \rangle - \langle a \rangle^2$ where $\langle a^2 \rangle = \langle \psi | \hat{A}^2 | \psi \rangle$. Such measurements are known as *projective* measurements and are a special case of the stronger version of the measurement postulate involving *Positive Operator-Valued Measures* (POVM).

1.1.4 The density matrix and POVM measurements

In practice it is usually impossible to define the precise quantum state of a physical system with a single ket $|x\rangle$. Rather, the system is in an unknown statistical mixture of several kets, a state fundamentally different from a superposition of the same kets. In this situation the state of the system is said to be *mixed* or *impure*. To describe this statistical mixture of different quantum states, we use the density matrix operator $\hat{\rho}$ which can be any positive semi-definite operator on $\mathcal{H}$. To describe a system which can be found in several states $\{|x_k\rangle\}_k$ with probabilities p_k, $\hat{\rho}$ is simply written as a weighted sum of projectors onto the respective vectors $|x_k\rangle$

$$\hat{\rho} = \sum_k p_k |x_k\rangle\langle x_k|. \tag{1.1.12}$$

Although written as a single sum, ρ is not in a diagonal form because nothing ensures that the vectors $\{|x_n\rangle\}$ are orthogonal. Therefore, the matrix representation of $\hat{\rho}$ in a discrete orthonormal basis $\{|n\rangle\}$ becomes

$$\hat{\rho} = \sum_{n,m} \rho_{n,m} |n\rangle\langle m|, \text{ where } \rho_{n,m} = \langle n | \hat{\rho} | m \rangle = \sum_k p_k \left(x_k^n\right)\left(x_k^m\right)^*, \tag{1.1.13}$$

with $x_k^n = \langle n | x_k \rangle$. Notice that $\hat{\rho}$ is non-negative and $\langle \psi | \hat{\rho} | \psi \rangle \geq 0$ for any ket $|\psi\rangle$), therefore, the set of all admissible density matrices is also the set of convex sums of projectors onto pure states. If our system is described by a density matrix $\hat{\rho}$, the average value $\langle a \rangle$ of the operator $\hat{A}$ is now expressed as the weighted sum of $\langle x_k | \hat{A} | x_k \rangle$ with weights p_k

$$\langle a \rangle = \sum_k p_k \langle x_k | \hat{A} | x_k \rangle. \tag{1.1.14}$$

Using the closure relation, we can rewrite $\langle a \rangle$ as

$$\langle a \rangle = \sum_k \langle x_k | \left(\sum_m |m\rangle\langle m| \right) \hat{A} \left(\sum_n |n\rangle\langle n| \right) |x_k\rangle = \sum_{n,m} \rho_{n,m} A_{m,n}, \tag{1.1.15}$$

which can be equivalently and concisely written with the *trace operation*

$$\langle a \rangle = \text{tr}[\hat{\rho}\hat{A}] = \sum_n \langle n| \left(\hat{\rho}\hat{A} \right) |n\rangle. \tag{1.1.16}$$

In the same way that a density matrix describes a mixed state, POVMs describe mixed measurements, or non-projective measurements. A POVM is a set of operators $\hat{O}_n = \hat{M}_n\hat{M}_n^\dagger$ following the closure relation $\sum_n \hat{O}_n = \hat{\mathbb{1}}$, where $\{\hat{M}_n\}$ is any set of operators on $\mathcal{H}$. The decomposition $\hat{O}_n = \hat{M}_n\hat{M}_n^\dagger$ ensures the positivity of $\hat{O}_n$

$$\forall x \in \mathcal{H}, \langle x|\hat{O}_n|x\rangle \geq 0, \tag{1.1.17}$$

a necessary condition for real-valued measurement outcomes. After a POVM measurement with outcome $\hat{O}_n$, the system in the original state $\hat{\rho}$ is projected onto the new states $\hat{\rho}'$

$$\hat{\rho}' = \hat{M}_n\hat{\rho}\hat{M}_n^\dagger/\text{tr}[\hat{\rho}\hat{O}_n]. \tag{1.1.18}$$

With only very general assumptions on the mathematical structure of the Hilbert spaces describing the quantum reality of physical systems, it is actually possible not to assume, but to deduce the measurement postulate and the formalism of the density matrix. Such an approach is based on the Gleason theorem [8, 36], on which more details can be found for example in [63].

1.1.5 Composite systems

Complex experimental systems can often only be described using a composite representation involving several Hilbert spaces $\mathcal{H}_1, \mathcal{H}_2, \ldots$ to take into account the physical reality of the laboratory. In this situation, the state of the system is described with a quantum state $|\psi\rangle$ which is an element of $\mathcal{H}$, the tensor product of all Hilbert spaces $\mathcal{H} = \mathcal{H}_1 \otimes \mathcal{H}_2 \otimes \ldots$ If $\{|n\rangle_i\}_{n \in \mathbb{N}}$ is an orthonormal basis of $\mathcal{H}_i$, then the canonical basis of $\mathcal{H}$ is

$$\{|n_1\rangle_1 \otimes |n_2\rangle_2 \otimes \ldots\}_{n_1 \in \mathbb{N}, n_2 \in \mathbb{N}, \ldots}, \quad \text{or} \quad \{|n_1, n_2, \ldots\rangle\}_{n_1 \in \mathbb{N}, n_2 \in \mathbb{N}, \ldots} \tag{1.1.19}$$

Although $\mathcal{H}$ itself can be written as a direct tensor product of its subspaces, due to the superposition principle its elements may be non-factorizable themselves over these subspaces, such as for example

$$|\psi\rangle = \frac{1}{\sqrt{2}} \left(|0\rangle_1|0\rangle_2 + |1\rangle_1|1\rangle_2 \right), \tag{1.1.20}$$

often written with the more simple notation $(|0,0\rangle + |1,1\rangle)/\sqrt{2}$. Such states are called entangled states because there is no valid representation of such non-local superposition states as products of separate states with their own individuality. Similarly, it is possible for density matrices to be non-factorizable entangled operators. In general, tracing out the degrees of liberty of one Hilbert space in a composite system leads to a representation of the latter state of the system with a mixed density matrix over the remaining reduced Hilbert space. For example if we trace $|\psi\rangle\langle\psi|$ on $\hat{\mathbb{1}}_2$ the identity operator of $\mathcal{H}_2$, we obtain

$$\text{tr}_2 \left(|\psi\rangle\langle\psi| \right) = \frac{1}{2} \left(\langle 0|_2|\psi\rangle\langle\psi|0\rangle_2 + \langle 1|_2|\psi\rangle\langle\psi|1\rangle_2 \right) = \frac{1}{2} \left(|0\rangle_1\langle 0|_1 + |1\rangle_1\langle 1|_1 \right) \tag{1.1.21}$$

Entangled states and entanglement is at the heart of quantum information processing, both as a way to achieve computational tasks, and also as the central cause of decoherence mechanisms due to spurious entanglement with the exterior environment. It turns out that entanglement is a very complex phenomenon far from full understanding For example, there are different ways a state can be entangled and there are different classes of entanglement, which depends, among other things, on the dimensionality of every sub-Hilbert spaces and the number of them. The classification of entanglement categories, especially for mixed states in infinite-dimensional Hilbert spaces, is still a work in progress.

1.2 Monomode quantum optics

In this section we review the usual theory of monomode quantum optics. Without being comprehensive, we limit ourselves to the relevant and necessary elements for the good understanding of the following chapters of this thesis. Further details about the full theory of quantum optics can be found in many textbooks, for example [26, 47, 34, 18, 31].

1.2.1 Quantum description of light

The description of light involves oscillating and propagating electrical $\vec{E}$ and magnetic $\vec{B}$ spatial vector fields, or in other words, electromagnetic waves. The dynamics of $\vec{E}$ and $\vec{B}$, that is the physics of light, is governed in classical physics by the famous Maxwell's equations. In the absence of electrical charges and currents, they are written in the microscopic form as the following set of differential equations

$$\vec{\nabla}.\vec{E}(x,y,z,t) = \vec{0}, \qquad \vec{\nabla} \times \vec{E}(x,y,z,t) = -\partial_t \vec{B}(x,y,z,t),$$
$$\vec{\nabla}.\vec{B}(x,y,z,t) = \vec{0}, \qquad \vec{\nabla} \times \vec{B}(x,y,z,t) = \tfrac{1}{c}\partial_t \vec{E}(x,y,z,t),$$
(1.2.1)

where c is the speed of light in the medium, $\times$ is the vector product and $\vec{\nabla} = (\partial_x, \partial_y, \partial_z)$. Literary, quantum optics could be limited to the standard procedure of quantification of the Maxwell's equations, but however, we are mainly interested in the consequences of this quantification. For a full description of the process of quantification of the electrical and magnetic fields, see [18, 34]. Here, we simply assume the validity of this process and present a shortcut to the result. For every independent mode l of frequency ω_l of the Maxwell's equations we associate a classical Hamiltonian functional H

$$H = \left(\sum_l \frac{1}{2m} p_l^2 + \frac{1}{2} m \omega_l^2 x_l^2 \right).$$
(1.2.2)

where x and p are the position and momentum variables. H describes the dynamic of a classical harmonic oscillator, a single mode of the Maxwell's equations, where a mode is a pair of (x, p) position and momentum variables whose dynamics is independent from the other modes. These modes naturally emerge in the spatio-temporal decomposition of the Maxwell's equation, for example with Fourier analysis. In this paragraph, these modes are plane waves, but we will see in Sec.1.4 that other spatio-temporal decompositions are valid, and can be especially relevant to complex geometric limit conditions happening for example inside optical resonators. The standard quantization procedure replaces the position and momentum variables by a pair of normalized non-commuting operators, themselves called the position and momentum operators or quadratures:

$$x_l \to \sqrt{\hbar/m\omega_l}\, \hat{x}_l, \text{ and } p_l \to \sqrt{\hbar m \omega_l}\, \hat{p}_l, \text{ with } [\hat{x}_l, \hat{p}_l] = i.$$
(1.2.3)

Looking at the original electrical field equation, we can understand the meaning of the mass parameter m as being

$$m = \epsilon_0/L^3,$$
(1.2.4)

where ϵ_0 is the so-called *vacuum permittivity* and L^3 is the quantification volume of the mode being looked at in the decomposition of the Maxwell's equations. For example for a quantified harmonic oscillator inside a cavity L^3 is simply the total volume of the spatial mode inside the cavity. The lower the quantification volume is the higher the mass of the oscillator becomes, and therefore the more energetic single quanta of light are. H becomes the Hamiltonian operator $\hat{H}$

which describes the self evolution of light waves without any external interactions and is written

$$H \rightarrow \hat{H} = \sum_l \frac{\hbar \omega_l}{2} \left(\hat{p}_l^2 + \hat{x}_l^2 \right). \tag{1.2.5}$$

We notice that the quantum description of light is essentially equivalent to the physics of the quantum harmonic oscillator. This remains true in the multi-mode analysis of light in Sec.1.4 where we study collections of independent quantum harmonic oscillators. In the remaining of this section we focus on a single quantized mode of the electrical field and write $H = \hbar \omega \left(\hat{x}^2 + \hat{p}^2 \right)/2$. Finally, from now on we use the unit system $\hbar = 1$.

1.2.2 Quadratures operators

We begin with the quadrature representation of the quantum harmonic oscillator. $\hat{x}$ and $\hat{p}$ are Hermitian operators and therefore they have two associated eigenvector basis $\{|x\rangle\}_{x \in \mathbb{R}}$ and $\{|p\rangle\}_{x \in \mathbb{R}}$. These basis are continuous and the eigenvectors relationship is written

$$\hat{x}|x\rangle = x|x\rangle, \quad \text{and} \quad \hat{p}|p\rangle = p|p\rangle, \tag{1.2.6}$$

with $x \in \mathbb{R}$ and $p \in \mathbb{R}$. Both basis are orthonormal so that $\langle x'|x \rangle = \delta(x - x')$ and $\langle p'|p \rangle = \delta(p - p')$. They also satisfy the closure relations

$$\frac{1}{\sqrt{2\pi}} \int dq |q\rangle\langle q| = \frac{1}{\sqrt{2\pi}} \int dp |p\rangle\langle p| = \hat{\mathbb{1}}. \tag{1.2.7}$$

Although a position ket $|x\rangle$ or momentum ket $|p\rangle$ is not a physical, normalized and measurable state, the quadrature representation is particularly useful to write the wave-function of the quantum state $|psi\rangle$ in the position or momentum domains with a single scalar product

$$\psi(q) = \langle q|\psi \rangle, \quad \text{and} \quad \tilde{\psi}(p) = \langle p|\psi \rangle, \tag{1.2.8}$$

where $\psi(q)$ and $\tilde{\psi}(p)$ constitute a Fourier pair

$$\tilde{\psi}(p) = \frac{1}{\sqrt{2\pi}} \int dq \psi(q) e^{-ipq}, \quad \text{and} \quad \psi(q) = \frac{1}{\sqrt{2\pi}} \int dp \tilde{\psi}(p) e^{+ipq}. \tag{1.2.9}$$

Plane waves $\langle p|q \rangle = \exp[-ipq]/\sqrt{2\pi}$ are a special case of wave function from which we can deduce that both basis $\{|x\rangle\}$ and $\{|p\rangle\}$ are images of each-other through the same isometric Fourier transform

$$|q\rangle = \frac{1}{\sqrt{2\pi}} \int e^{-ipq}|p\rangle dp, \quad \text{and} |p\rangle = \frac{1}{\sqrt{2\pi}} \int e^{+iqp}|q\rangle dq. \tag{1.2.10}$$

Finally, we can define translation operators in position or in momentum. If we define the operator $\hat{T}_{\hat{x}}(\lambda) = e^{-i\lambda \hat{p}}$ and then express the commutator $\left[\hat{x}, \hat{T}_{\hat{x}}(\lambda) \right]$ with $\hat{x}$ in the following form

$$\hat{x}\hat{T}_{\hat{x}}(\lambda)|0\rangle = \hat{T}_{\hat{x}}(\lambda)(\lambda + \hat{x})|0\rangle = \lambda \hat{T}_{\hat{x}}(\lambda)|0\rangle, \tag{1.2.11}$$

we deduce the translation in position relationship $\hat{T}_{\hat{x}}(q)|0\rangle_x = |q\rangle$ where $|0\rangle_x$ is the quantum state of position zero. In the same fashion if we define $\hat{T}_{\hat{p}}(\mu) = e^{+i\mu \hat{x}}$ we obtain the translation in momentum relationship $\hat{T}_{\hat{p}}(p)|0\rangle = e^{+ip\hat{x}}|0\rangle_p = |p\rangle$. These two operators are important in the theory of teleportation in Chap.**??** and can be implemented experimentally almost perfectly using highly reflecting mirrors and auxiliary light beams.
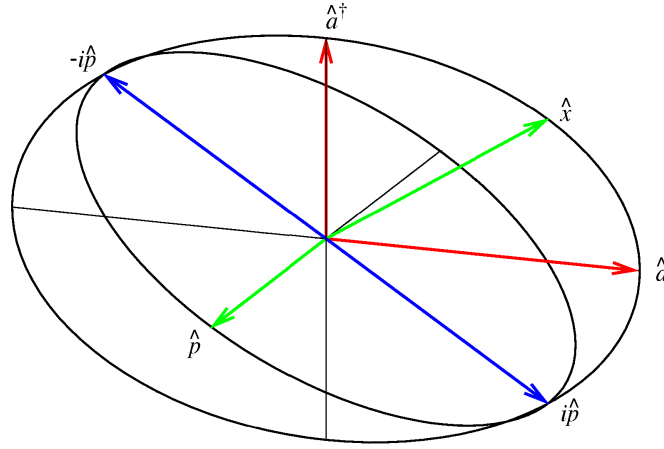
Figure 1.1: Relation between the $(\hat{x}, \hat{p})$ basis and the $(\hat{a}, \hat{a}^\dagger)$ basis. The complex multiplication by i is represented as a $\pi/2$ rotation around the $\hat{x}$ axis.

1.2.3 Photon number states

If we introduce the operator $\hat{a}$ and its Hermitian adjoint $\hat{a}^\dagger$, respectively called the *annihilation* and *creation* operators, by the relations

$$\hat{a} = (\hat{q} + i\hat{p})/\sqrt{2}, \text{ and } \hat{a}^\dagger = (\hat{q} - i\hat{p})/\sqrt{2}, \qquad (1.2.12)$$

$\hat{H}$ can be rewritten in the factorized form

$$\hat{H} = \hbar\omega \left(\hat{a}^\dagger \hat{a} + \frac{1}{2} \right) = \hbar\omega \left(\hat{n} + \frac{1}{2} \right). \qquad (1.2.13)$$

The operator $\hat{n} = \hat{a}^\dagger \hat{a}$ is an Hermitian operator whose eigenvectors are written $|n\rangle$, with eigenvalues n. With the commutator relation $[\hat{a}, \hat{a}^\dagger] = 1$ it is possible to show that

$$\hat{a}|n\rangle = \sqrt{n}|n-1\rangle, \text{ and } \hat{a}^\dagger|n\rangle = \sqrt{n+1}|n+1\rangle, \qquad (1.2.14)$$

from which we deduce that the admissible eigenvalues n are positive integer only, starting from 0. This integer spectrum is interpreted as the elementary particles of light, called photons, and $\hat{n}$ is therefore called the *photon number* operator. For instance, $|3\rangle$ represents the state of exactly 3 energy quanta of light, while $|1\rangle$ is the state of exactly one quantum of light. $\{|n\rangle\}$ is called the photon basis, or the basis of photon number states. In quantum optics, it is the most commonly used representation of the density matrix $\hat{\rho}$. The eigenvector $|0\rangle$ of eigenvalue $\hat{n}|0\rangle = 0$ is called the *vacuum* state and also satisfies $\hat{a}|0\rangle = 0$. This translates into the differential equation $(q + \partial_q)\psi_0(q) = 0$, where $\psi_0(q) = \langle q|0\rangle$ and whose unique solution is

$$\psi_0(q) = \exp[-q^2/2]/\pi^{1/4}. \qquad (1.2.15)$$

Any photon number state $|n\rangle$ can be written from the vacuum state $|0\rangle$ with successive iterations of the creation operator $\hat{a}^\dagger$

$$|n\rangle = \frac{(\hat{a}^\dagger)^n}{\sqrt{n!}}|0\rangle \qquad (1.2.16)$$

The wave-function $\psi_n(q) = \langle q|n\rangle$ of $|n\rangle$ can be expressed as

$$\psi_n(q) = H_n(q)\psi_0(q)/\sqrt{2^n n!} \qquad (1.2.17)$$

where H_n is the nth order Hermite polynomial. The photon basis is also orthonormal and $\langle n|m \rangle = \delta_n^m$. It is complete and satisfies the closure relation $\sum_n |n\rangle\langle n| = \hat{\mathbb{1}}$. Finally, the wave-functions $\psi_n(q)$ of the photon basis have the interesting property of being the eigenstates of the Fourier transform. Therefore for any n ψ_n has the same algebraic expression in the position and momentum basis. In other words, photon number states give no information at all about the quadrature angle, which can be seen as the conjugate variable to $\hat{n}$, although this definition is mathematically fragile. Since the photon number states $\hat{n}$ are also eigenstates of the Hamiltonian $\hat{H}$, it is natural that this symmetry is also found in the expression of $\hat{H}$ in Eq.(1.2.5).
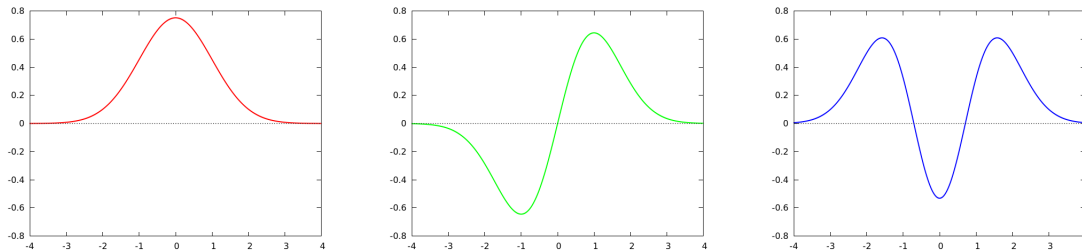

Figure 1.2: Examples of photon number state wave-functions. Left: $|0\rangle$. Center: $|1\rangle$. Right: $|2\rangle$.

1.2.4 Phase shifting

The phase shifter operator $\hat{U}_\theta$ is defined by

$$\hat{U}_\theta = e^{-i\theta\hat{n}}, \tag{1.2.18}$$

with $\theta \in [0, 2\pi[$. Its action on $\hat{a}$ is

$$\hat{U}_\theta^\dagger \hat{a} \hat{U}_\theta = \hat{a}e^{-i\theta}, \tag{1.2.19}$$

and can be calculated by deriving $\hat{U}_\theta$ with respect to θ and solving the differential equation $\partial_\theta \hat{U}_\theta^\dagger \hat{a} \hat{U}_\theta = i\hat{U}_\theta^\dagger [\hat{n}, \hat{a}] \hat{U}_\theta = -\hat{U}_\theta^\dagger \hat{a} \hat{U}_\theta$. In the position and momentum basis, the transformation becomes

$$\hat{x}_\theta = \hat{U}_\theta^\dagger \hat{x} \hat{U}_\theta = \cos\theta \hat{x} + \sin\theta \hat{p}, \quad \text{and} \quad \hat{p}_\theta = \hat{U}_\theta^\dagger \hat{p} \hat{U}_\theta = \cos\theta \hat{p} - \sin\theta \hat{x}. \tag{1.2.20}$$

The phase shifter operator is simply a rotation of the quadrature basis which can be used to define infinitely many quadrature operators basis $(\hat{x}_\theta, \hat{p}_\theta)$. It is important in the theory of optical homodyne tomography and appears in the expression of the Radon transform (see Sec. **??**). Also, for $\theta = \pi/2$, $\hat{U}_{\pi/2}$ is simply the Fourier operator which transforms $\hat{x}$ to $\hat{p}$ and $\hat{p}$ to $-\hat{x}$. With the phase shifter operator, it is possible to extend the definition of the wave-function to any quadrature angle θ with the exression $\psi(q, \theta) = \langle q_\theta|\psi\rangle$ where $|q_\theta\rangle = \hat{U}_\theta^\dagger|q\rangle$. The relation between the original wave-function $\psi(q)$ in the position basis and the new wave-function in the rotated quadrature is similar to a generalized Fourier transform. For the photon number state basis, this rotation simply takes the form of an additional phase factor

$$\psi_n(q, \theta) = H_n(q)\psi_0(q)e^{-in\theta}/\sqrt{2^n n!}. \tag{1.2.21}$$

1.2.5 Coherent states

We introduce the unitary operator $\hat{D}_\alpha$, where $\alpha = \frac{1}{\sqrt{2}}(q + ip)$ is any complex number, with the expression

$$\hat{D}_\alpha = e^{\alpha^*\hat{a} - \alpha\hat{a}^\dagger} = e^{ip_0\hat{q} - iq_0\hat{p}}. \tag{1.2.22}$$
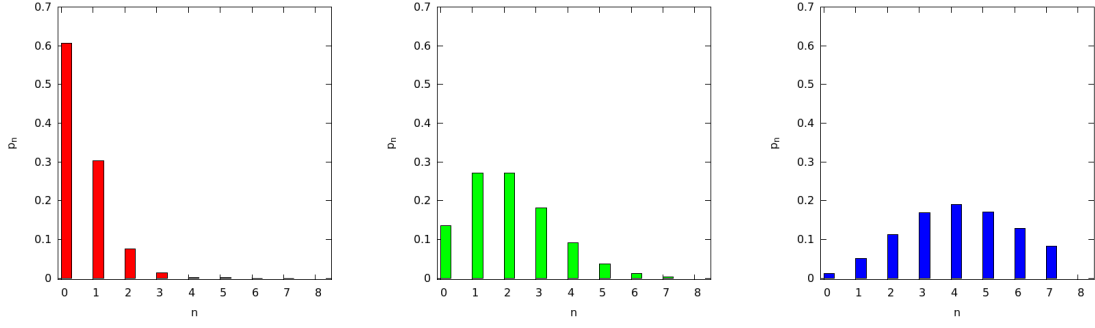
Figure 1.3: Example of photon number statistics for coherent states $|\alpha\rangle$. Left, $\alpha = 1$. Center, $\alpha = 2$. Right, $\alpha = 3$.

The Hermitian adjoint $\hat{D}_\alpha^\dagger$ of $\hat{D}_\alpha$ is $\hat{D}_{-\alpha}$. $\hat{D}_\alpha$ is called the *displacement* operator because its action on the annihilation operator $\hat{a}$ is similar to a translation by the complex amplitude α

$$\hat{D}_\alpha^\dagger \hat{a} \hat{D}_\alpha = \hat{a} + \alpha. \tag{1.2.23}$$

Using the Baker-Hausdorff formula

$$e^{\hat{A}+\hat{B}} = e^{\hat{A}} e^{\hat{B}} e^{-[\hat{A},\hat{B}]} = e^{\hat{B}} e^{\hat{A}} e^{[\hat{A},\hat{B}]}, \tag{1.2.24}$$

we can decompose the displacement operator in the quadrature basis

$$\hat{D}_\alpha = e^{ip_0 q_0/2} e^{-iq_0 \hat{p}} e^{-ip_0 \hat{q}} = e^{ip_0 q_0/2} e^{-ip_0 \hat{q}} e^{iq_0 \hat{p}}, \tag{1.2.25}$$

and deduce its effect on $\hat{x}$ and $\hat{p}$

$$\hat{D}_\alpha^\dagger \hat{q} \hat{D}_\alpha = \hat{q} + q, \quad \text{and} \quad \hat{D}_\alpha^\dagger \hat{p} \hat{D}_\alpha = \hat{p} + p. \tag{1.2.26}$$

Displacement operators can be concatenated in a vector-like fashion

$$\hat{D}_\alpha \hat{D}_\beta = \hat{D}_{\alpha+\beta} \, e^{-\text{Re}(\alpha\beta^*)}. \tag{1.2.27}$$

We now define the set of coherent states $\{|\alpha\rangle\}_{\alpha\in\mathbb{C}}$ for any complex number α as the set of displaced vacuum states

$$|\alpha\rangle = \hat{D}_\alpha |0\rangle. \tag{1.2.28}$$

With Eq.(1.2.23), we deduce that coherent states are the eigenstates of the annihilation operator $\hat{a}$

$$\hat{a}|\alpha\rangle = \alpha|\alpha\rangle. \tag{1.2.29}$$

The wave-function $\psi_\alpha(x) = \langle x|\alpha\rangle$ of the coherent state of amplitude α can be derived from the vacuum state wave-function $\psi_0(x)$

$$\psi_\alpha(x) = \langle x|\hat{D}_\alpha|0\rangle = e^{ipx-ipq/2}\psi_0(x - q). \tag{1.2.30}$$

We deduce from the last equation the overlap formula of two coherent states $|\alpha\rangle$ and $|\alpha'\rangle$

$$\langle\alpha|\alpha'\rangle = \exp\left(-\frac{|\alpha|^2 + |\alpha'|^2}{2} + \alpha'\alpha^*\right). \tag{1.2.31}$$

We notice that coherent states are not strictly orthogonal. It turns out that the coherent state basis is over-complete and does not exactly follow the closure relation, but rather

$$\int d^2\alpha |\alpha\rangle\langle\alpha| = 2\pi. \tag{1.2.32}$$

With Eq.(1.2.16), we deduce the photon number decomposition of $|\alpha\rangle$

$$|\alpha\rangle = e^{-|\alpha|^2/2} \sum_n \frac{\alpha^n}{\sqrt{n!}} |n\rangle. \tag{1.2.33}$$

We notice that the probability $p_\alpha(n)$ of measuring n photons in $|\alpha\rangle$ is equal to $|\alpha|^{2n} \exp(-|\alpha|^2)/n!$ and therefore follows a Poisson distribution. The average photon number $\langle n \rangle$ of $|\alpha\rangle$ is simply $|\alpha|^2$. The set of coherent states $\{|\alpha\rangle\}_{\alpha\in\mathbb{C}}$ has played an important historical role in the precise definition of the quantum theory of light by Glauber and others[47].
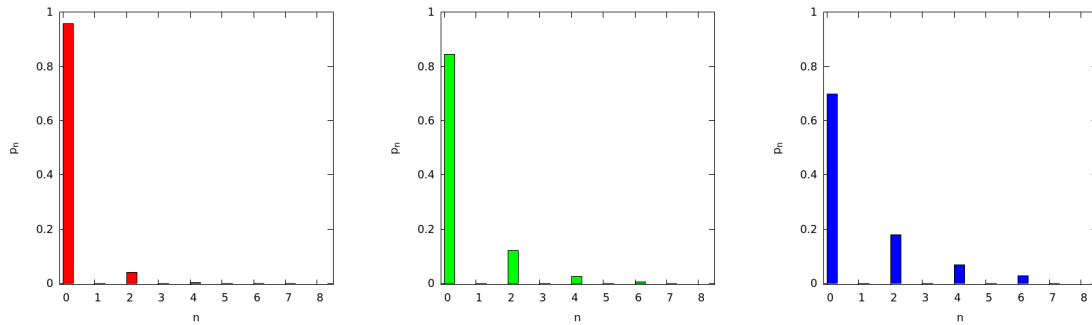
1.2.6 Squeezed states

Figure 1.4: Example of photon number statistics for squeezed vacuum states $\hat{S}_s|0\rangle$. Left, $s = 0.3$. Center, $s = 0.6$ Right, $s = 0.9$.

We introduce the unitary *squeezing* operator $\hat{S}_s$, where $s \in \mathbb{R}$ is a real parameter, with the expression

$$\hat{S}_s = \exp\left[\frac{s}{2}((\hat{a})^2 - (\hat{a}^\dagger)^2)\right]. \tag{1.2.34}$$

We notice that $\hat{S}_s^{-1} = \hat{S}_{-s}$. With its definition similar to the displacement operator $\hat{D}_\alpha$, the squeezing operator is also called the *two-photon displacement* operator. With the identity

$$e^{-\hat{B}}\hat{A}e^{\hat{B}} = \hat{A} + \left[\hat{B}, \hat{A}\right] + \frac{1}{2!}\left[\hat{B}, \left[\hat{B}, \hat{A}\right]\right] + \dots, \tag{1.2.35}$$

we deduce the effect of $\hat{S}_s$ on $\hat{a}$

$$\hat{S}_s^\dagger \hat{a} \hat{S}_s = \cosh(s)\hat{a} - \sinh(s)\hat{a}^\dagger \tag{1.2.36}$$

and its characterization in the quadrature basis

$$\hat{S}_s^\dagger \hat{q} \hat{S}_s = e^{-s}\hat{q}, \quad \text{and} \quad \hat{S}_s^\dagger \hat{p} \hat{S}_s = e^{+s}\hat{p}. \tag{1.2.37}$$

The main property of the squeezing operator is to reduce the variance of one quadrature operator beyond the standard quantum noise level of the vacuum state, while the standard deviation of the orthogonal quadrature necessarily increases so that the Heisenberg inequalities are preserved

$$\langle 0|\hat{S}_s^\dagger \hat{x}^2 \hat{S}_s|0\rangle = e^{-2s}/2, \quad \text{and} \quad \langle 0|\hat{S}_s^\dagger \hat{p}^2 \hat{S}_s|0\rangle = e^{+2s}/2. \tag{1.2.38}$$

A state $\hat{S}_s|0\rangle$ is called a *squeezed vacuum* state. It is written in the photon basis with the decomposition

$$\hat{S}_s|0\rangle = \left(1 - \lambda^2\right)^{1/4} \sum_{n=0} \frac{\sqrt{2n!}}{n!} \left(\lambda/2\right)^n |2n\rangle, \tag{1.2.39}$$

with $\lambda = \tanh(s)$. The mean photon number of a squeezed vacuum is $\langle\hat{n}\rangle = \sinh^2(s) \neq 0$. Such a squeezed quantum state can be produced with interaction Hamiltonian operators of the form $\propto (\hat{a})^2 - (\hat{a}^\dagger)^2$ which can be experimentally achieved with non-linear optics setups and for example the process of parametric-down conversion. The squeezed vacuum state is the primary resource of many quantum algorithms and circuits with applications to continuous variable quantum information processing. For instance, linear optics and ancilla squeezed vacuum states are the necessary and sufficient resources for Gaussian operations, such as teleportation or cluster state computation. Furthermore, we will see in Chap.**??** that squeezed vacuum states can also be used to generate non-Gaussian non-classical states by exploiting two-photons correlations and photon counting devices.
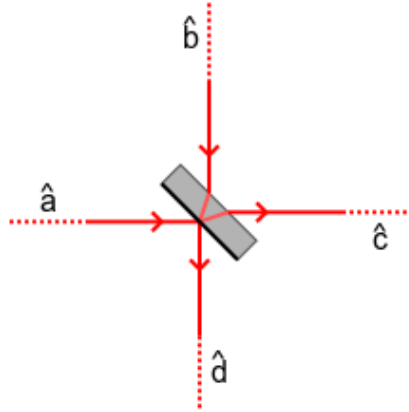
1.2.7   Beam splitters

Figure 1.5: A beam-splitter with its input modes $\hat{a}$, $\hat{b}$ and output modes $\hat{c}$, $\hat{d}$.

A beam-splitter is a 2 input ports 2 output ports passive device which stochastically splits incoming light on the input port and redistributes it towards the output port. It is a simple and basic device, yet crucial for the field of quantum optics and the generation of quantum interferences with light. We consider two classical amplitudes E_1, E_2 at the input of a beam-splitter, whose two output electrical fields are E_3 and E_4. The beam-splitter equations are written

$$E_3 = \cos\theta\, E_1 - \sin\theta\, E_2, \tag{1.2.40}$$
$$E_4 = \cos\theta\, E_2 + \sin\theta\, E_1, \tag{1.2.41}$$

where $\theta \in [0, 2\pi[$ is the amount of splitting of the beam-splitter. $\cos(\theta)$ and $\sin(\theta)$ are respectively the transmission and reflection coefficients T and R, in amplitude. The cosine and sine formulation automatically verifies the energy conservation rule $T^2 + R^2 = 1$. Eqs.(1.2.40) can be written as a matrix transformation

$$\begin{pmatrix} E_3 \\ E_4 \end{pmatrix} = B_\theta \begin{pmatrix} E_1 \\ E_2 \end{pmatrix}, \text{ with } B_\theta = \begin{pmatrix} \cos\theta & -\sin\theta \\ \sin\theta & \cos\theta \end{pmatrix}. \tag{1.2.42}$$

Since the quantization of the electrical field preserve the linear character of the Maxwell's equations, the effect of the beam-splitter on annihilation operators is written

$$\hat{c} = \cos\theta\,\hat{a} - \sin\theta\,\hat{b}, \tag{1.2.43}$$

$$\hat{d} = \cos\theta\,\hat{b} + \sin\theta\,\hat{a}, \tag{1.2.44}$$

where $\hat{a}$, $\hat{b}$, $\hat{c}$ and $\hat{d}$ are associated respectively to E_1, E_2, E_3 and E_4. These two equations can also takes the matrix form

$$\begin{pmatrix} \hat{c} \\ \hat{d} \end{pmatrix} = B_\theta \begin{pmatrix} \hat{a} \\ \hat{b} \end{pmatrix}. \tag{1.2.45}$$

which preserves commutators. We notice that B_θ is a unitary matrix and that $B_\theta^{-1} = B_\theta^T = B_{-\theta}$.

Heisenberg picture

We are looking for a unitary operator $\hat{B}_\theta$ which describes in the Heisenberg picture the beam-splitter input/output transformation of Eq.(1.2.43) in the following way

$$\hat{B}_\theta \begin{pmatrix} \hat{a} \\ \hat{b} \end{pmatrix} \hat{B}_\theta^\dagger = B_\theta \begin{pmatrix} \hat{a} \\ \hat{b} \end{pmatrix}. \tag{1.2.46}$$

As some other operators we saw in Secs.1.2.4, 1.2.5 and 1.2.6, $\hat{B}_\theta$ has the simple exponential formulation

$$\hat{B}_\theta = \exp\left[\theta\left(\hat{a}^\dagger\hat{b} - \hat{b}^\dagger\hat{a}\right)\right]. \tag{1.2.47}$$

When going through calculations with this specific expression of the beam-splitter operation in the Heisenberg picture, it is important to keep track of the current basis, that is, if the current operators $\hat{a}$ and $\hat{b}$ represent the initial input modes or the output modes after the beam-splitter.

Schroedinger picture

In the Schroedinger picture, $\hat{B}_\theta$ is described by its action on the density matrix $\hat{\rho}$ through the expression $\hat{\rho}' = \hat{B}_\theta^\dagger\hat{\rho}\hat{B}_\theta$ which translates in the photon basis to

$$\hat{B}_\theta^\dagger|n,m\rangle = \frac{1}{\sqrt{n!m!}}\hat{B}_\theta^\dagger a^{\dagger n}b^{\dagger m}\hat{B}_\theta|0,0\rangle \tag{1.2.48}$$

with $\hat{B}_\theta^\dagger|0,0\rangle = |0,0\rangle$. The above expression can be further decomposed into

$$\hat{B}_\theta^\dagger|n,m\rangle = \sum_{k=0}^{n}\sum_{l=0}^{m} B_\theta(n,m,k,l)|k+l,n+m-k-l\rangle \tag{1.2.49}$$

with the coefficients $B_\theta(n,m,k,l)$ given by

$$B_\theta(n,m,k,l) = (-1)^l \begin{pmatrix} n \\ k \end{pmatrix}\begin{pmatrix} m \\ l \end{pmatrix}\sqrt{\begin{pmatrix} n+m \\ n \end{pmatrix}\Big/\begin{pmatrix} n+m \\ k+l \end{pmatrix}}(\cos\theta)^{m+k-l}(\sin\theta)^{n+l-k} \tag{1.2.50}$$

In the special case $m = 0$ where the second input port of the beam-splitter is in the vacuum state $|0\rangle$, Eq.(1.2.49) simplifies itself to

$$\hat{B}_\theta^\dagger|n,0\rangle = \sum_{k=0}^{n}\sqrt{\begin{pmatrix} n \\ k \end{pmatrix}}(\cos\theta)^k(\sin\theta)^{n-k}|k,n-k\rangle \tag{1.2.51}$$

which exactly follows a binomial distribution. In other words, n photon at the input of a beam-splitter are randomly split to both output ports with probability $(\cos\theta)^2$, independently from each others. This is the stochastic nature of the beam-splitter splitting and quite naturally we understand that a beam-splitter can be thought of purely in term of classical physics to the difference that it preserves quantum coherence and quantum superposition.
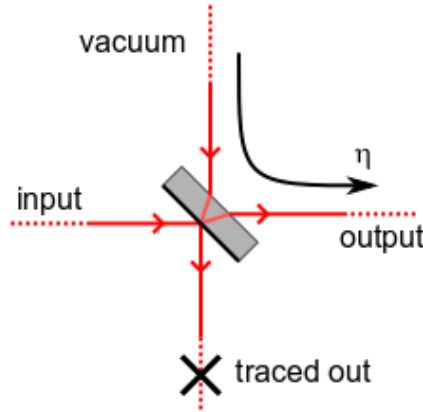
Model of linear losses

Figure 1.6: Representation of the beam-splitter model of linear amplitude lossses.

In practice, quantum states of light generated in the laboratory suffer from experimental imperfections, and only a density matrix representation can faithfully describe such states. One of the main sources of imperfection is propagation losses, which can be easily modeled with the help of the above beam-splitter formalism. The central idea of the model is to assume that losses are exactly proportional to the incoming amplitude of light. In other words, if a coherent state $|\alpha\rangle$ enters our system with an intensity transmission efficiency η, the output is the coherent state $|\sqrt{\eta}\alpha\rangle$. In the Heisenberg picture, this can be described by the transformation

$$\hat{a}' = \sqrt{\eta}\hat{a} + \sqrt{1-\eta}\hat{b}, \tag{1.2.52}$$

where $\hat{b}$ is an auxiliary mode used to take away the energy lost in $|\sqrt{\eta}\alpha\rangle$. This relationship is exactly similar to Eqs.(1.2.43), provided $\cos\theta = \sqrt{\eta}$, and this model of amplitude dumping is equivalent to the simple picture of a fictitious beam-splitter with a transmission coefficient $\sqrt{\eta}$. While the input quantum state suffers losses through the beam-splitter, the other input port of the beam-splitter is assumed to be $|0\rangle$. After the fictitious beam-splitter, the quantum degrees of liberty of the output mode taking away the lost fraction of the light are traced out. In the density matrix picture, if $\hat{\rho}$ is the input state in mode 1, the output state $\hat{\rho}'$ in mode 3 can be expressed as

$$\hat{\rho}' = \mathrm{tr}_4\left(\hat{B}_\theta^\dagger \hat{\rho}\otimes|0\rangle_2\langle 0|_2\hat{B}_\theta\right) \tag{1.2.53}$$

which can be detailed in the photon basis using Eq.(1.2.51). We notice that because the trace operation is partial only, we cannot change $\hat{B}_\theta^\dagger\hat{\rho}\otimes|0\rangle\langle 0|\hat{B}_\theta$ to $\hat{\rho}\otimes|0\rangle\langle 0|$ inside it with the circular trace formulae. In the next section we see how this model expresses itself in phase-space.

1.3   Phase space representations

In Sec.1.1, we have seen that the density matrix is easily represented in the photon number basis. Instead of using a discrete representation $\hat{\rho} = \sum \rho_{n,m} |n\rangle\langle m|$, we are interested in this section in continuous representations $f(\alpha)$ of quantum states in phase space, which for example could look like $\int d^2\alpha f(\alpha)|\alpha\rangle\langle\alpha|$. These continuous representation are known as *quasi-probability distributions* and it turns out there is infinitely many way to define such representations f. We will focus especially on the Wigner function which is the most convenient continuous representation to manipulate theoretically and to measure experimentally. A good reference for more details on the origin of most useful phase-space quasi-probability distributions and their relations to each other is [47]. [26] contains also an interesting summary of the most useful properties of the main phase-space distributions. More details about the Wigner function only can be found in [34].

1.3.1   The Wigner function

The Wigner function was introduced by Wigner in [5] to describe corrections to classical thermo-dynamic equilibrium imposed by the still quite young theory of quantum mechanics. It is uniquely defined from the density matrix $\hat{\rho}$ by the linear relation

$$W(q,p) = \frac{1}{2\pi} \int_{-\infty}^{+\infty} e^{ipx}\langle q - \frac{x}{2}|\hat{\rho}|q + \frac{x}{2}\rangle dx. \tag{1.3.1}$$

Here, q and p represent classical values of the phase space position and momentum variables. We will also sometime write $W(\alpha)$ with $\alpha = (q+ip)/\sqrt{2}$. The Wigner function has many interesting properties which make it a privileged tool of analysis in quantum optics. From its definition we notice that W is real and $W(x,p)^* = W(x,p)$. Furthermore, $W(x,p)$ is always definite. We will see in paragraph 1.3.1 that in addition, the Wigner function has a partial interpretation in term of probability distributions, which together with the two above properties, makes it the numerical representation of choice for quantum states. With Eq.(1.2.15) and the definition (1.3.1), we easily obtain the Wigner function $W_{|0\rangle}(q,p)$ of the vacuum state $|0\rangle$

$$W_{|0\rangle}(q,p) = e^{-q^2-p^2}/\pi. \tag{1.3.2}$$

$W_{|1\rangle}(q,p)$ is another Wigner function that we will use in Chap.**??** and Chap.**??**

$$W_{|1\rangle}(q,p) = \frac{2}{\pi}\left(q^2 + p^2 - 1/2\right)e^{-q^2-p^2}. \tag{1.3.3}$$

Finally, the definition of Eq.(1.3.1) can be extended into a two-mode Wigner function $W_{1,2}(q_1,p_1,q_2,p_2)$ describing the sub-systems $(\hat{q}_1,\hat{p}_1)$ and $(\hat{q}_2,\hat{p}_2)$. If the total density matrix $\hat{\rho}_{1,2}$ can be factorized into $\hat{\rho}_1 \otimes \hat{\rho}_2$, then $W_{1,2}(q_1,p_1,q_2,p_2)$ will also factorize into $W_1(q_1,p_1)W_2(q_2,p_2)$. In general, this is not the case, and the Wigner function can also be used to account for any kind of entanglement.

Phase space transformations

Several unitary operators introduced in Sec.1.2 have simple and interesting expressions in phase space with the Wigner function. If we displace the density matrix $\hat{\rho}$ whose Wigner function is $W(q,p)$ by $\alpha = (q_0 + ip_0)/\sqrt{2}$, then the Wigner function $W'(q,p)$ of $\hat{\rho}' = \hat{D}_\alpha \hat{\rho} \hat{D}_\alpha^\dagger$ is written

$$W'(q,p) = \frac{1}{2\pi}\int_{-\infty}^{+\infty} e^{ipx}\langle q - \frac{x}{2}|\hat{D}_\alpha\hat{\rho}\hat{D}_\alpha^\dagger|q + \frac{x}{2}\rangle dx \tag{1.3.4}$$

$$= \frac{1}{2\pi}\int_{-\infty}^{+\infty} e^{i(p-p_0)x}\langle (q-q_0) - \frac{x}{2}|\hat{\rho}|(q-q_0) + \frac{x}{2}\rangle dx. \tag{1.3.5}$$
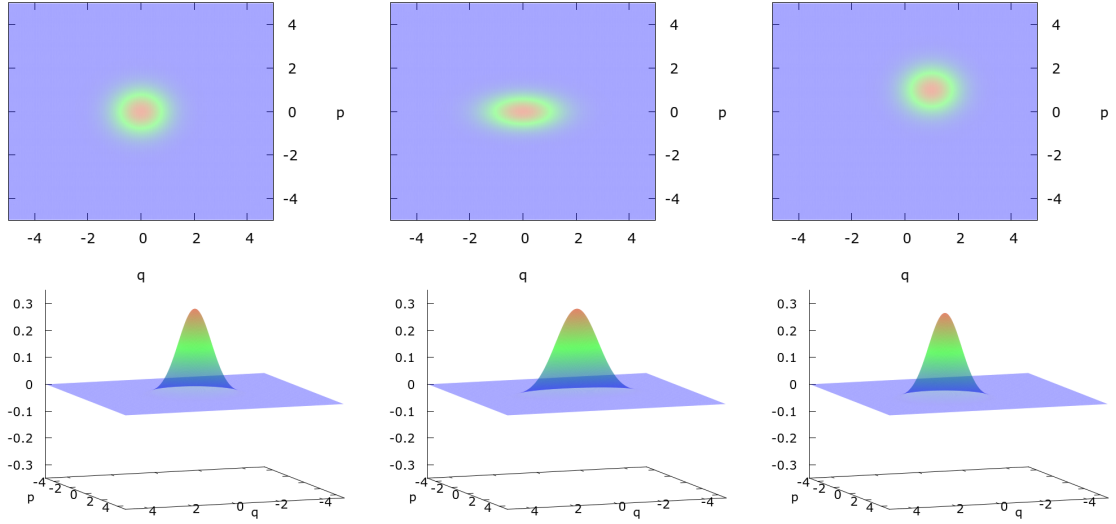
Figure 1.7: Examples of common Gaussian Wigner functions. Left: vacuum state $|0\rangle$. Center: squeezed vacuum state $\hat{S}_s|0\rangle$ with $s = 0.3$. Right: coherent state $|\alpha\rangle$ with $\alpha = (1+i)/\sqrt{2}$.

The action of the displacement operator is a simple translation in phase space

$$W(x,p) \xrightarrow{\hat{D}_\alpha} W'(x,p) = W(x - x_0, p - p_0). \tag{1.3.6}$$

Therefore, the Wigner function W_α of the coherent state $|\alpha\rangle$ is simply $W_{|0\rangle}(q - q_0, p - p_0)$. In the same fashion, if we apply the squeezing operation $\hat{\rho} \to \hat{\rho}' = \hat{S}_s\hat{\rho}\hat{S}_s^\dagger$, then the Wigner function is transformed as

$$W(q,p) \xrightarrow{\hat{S}_s} W'(q,p) = W(e^{+s}q, e^{-s}p). \tag{1.3.7}$$

We immediately deduce the Wigner function $W_{\hat{S}_s|0\rangle}(q,p)$ of a squeezed vacuum as

$$W_{\hat{S}_s|0\rangle}(q,p) = W_{|0\rangle}(e^{+s}q, e^{-s}p) = \exp\left[-e^{+2s}x^2 - e^{-2s}p^2\right]/\pi. \tag{1.3.8}$$

The phase shifting operator $\hat{U}_\theta$ changes the Wigner function as

$$W(q,p) \xrightarrow{\hat{U}_\theta} W'(q,p) = W(\cos\theta q - \sin\theta p, \cos\theta p + \sin\theta q). \tag{1.3.9}$$

Finally, the beam splitter operator $\hat{B}_\theta$ will changes the 2-mode Wigner function $W_{1,2}(q_1, p_1, q_2, p_2)$ into

$$W_{1,2}(q_1, p_1, q_2, p_2) \xrightarrow{\hat{B}_\theta} W'_{1,2}(q_1, p_1, q_2, p_2) = W_{1,2}(q'_1, p'_1, q'_2, p'_2). \tag{1.3.10}$$

with

$$\begin{pmatrix} q'_1 \\ -q'_2 \end{pmatrix} = B_\theta \begin{pmatrix} q_1 \\ q_2 \end{pmatrix}, \quad \text{and} \quad \begin{pmatrix} p'_1 \\ -p'_2 \end{pmatrix} = B_\theta \begin{pmatrix} p_1 \\ p_2 \end{pmatrix}. \tag{1.3.11}$$

Photon basis decomposition

If we write down the density matrix in the photon representation $\hat{\rho} = \sum_{n,m} \rho_{n,m}|n\rangle\langle m|$, thanks to the linearity of Eq.(1.3.1), we see that

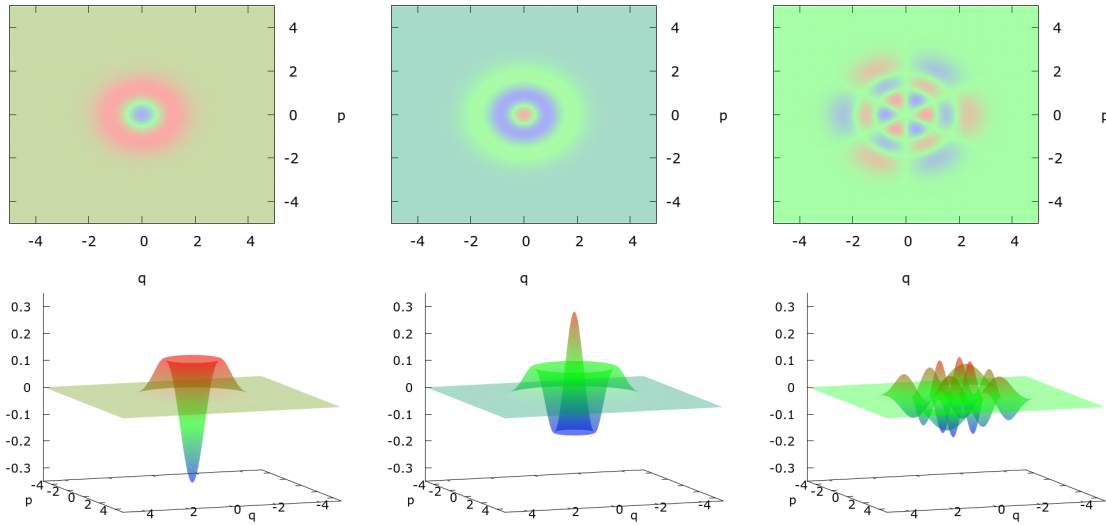$$W(q,p) = \sum_{n,m} \rho_{n,m} W_{n,m}(q,p), \tag{1.3.12}$$

Figure 1.8: Examples of photon numbers Wigner functions. Left: $|1\rangle$. Center: $|2\rangle$. Right: real part of $|2\rangle\langle 5| + |5\rangle\langle 2|$.

where the functions $W_{n,m}(q,p)$, known as the Moyal functions of the harmonic oscillators [34], are defined as

$$W_{n,m}(q,p) = \frac{1}{2\pi} \int_{-\infty}^{+\infty} e^{ipx} \langle q - \frac{x}{2}|n\rangle\langle m|q + \frac{x}{2}\rangle dx, \qquad (1.3.13)$$

and can be expressed for $n \geq m$ with the Laguerre polynomials $L_s^t(y)$ as

$$W_{n,m}(q,p) = (-1)^m \left(\sqrt{2}(q - ip)\right)^{n-m} \sqrt{m!/n!}\, L_m^{n-m}\left(2(q^2 + p^2)\right) W_{|0\rangle}(q,p), \qquad (1.3.14)$$

with the symmetric expression for $m \geq n$. Because $|n\rangle\langle m|$ is not a physical state when $n \neq m$, $W_{n,m}(x,p)$ are complex functions, and we have the symmetry relation $W_{n,m}(q,p) = W_{m,n}^*(q,p)$. We notice that $W_{n,m}(0,0) = (-1)^n \delta_n^m/\pi$, therefore we deduce the formula

$$W(0,0) = \frac{1}{\pi} \sum_n (-1)^n \rho_{n,n}. \qquad (1.3.15)$$

$W(0,0)$ is usually called the *negativity* of the Wigner function. It is the central figure of merit for generation and teleportation of non-Gaussian states in Chaps.**??** and **??** to evaluate the quality of experimental non-Gaussian states. In Chap.**??**, we will see how to evaluate the negativity $W(0,0)$ with the process of quantum tomography.

Link with the marginal distribution

It is easy to show from the definition 1.3.1 of the Wigner function that

$$\int dp\, W(q,p) = \langle q|\hat{\rho}|q\rangle. \qquad (1.3.16)$$

Furthermore we have seen in Eq.1.3.9 that the transformation $\hat{\rho}' = U_\theta \hat{\rho} U_\theta^\dagger$ changes the Wigner function to $W'(q,p) = W(q\cos\theta - p\sin\theta, p\cos\theta + q\sin\theta)$. Therefore, we also obtain after a $\pi/2$ rotation in phase space

$$\int dq\, W(q,p) = \langle p|\hat{\rho}|p\rangle. \qquad (1.3.17)$$

Finally with further rotations, we can obtain the probability distribution of the position and momentum quadratures in any angular basis

$$\langle q|U_\theta \hat{\rho} U_\theta^\dagger|q\rangle = \int dp W(q\cos\theta - p\sin\theta, p\cos\theta + q\sin\theta). \tag{1.3.18}$$

The LHS of Eq.(1.3.18) is interpreted as the probability distribution of the position quadrature in the angular basis θ according to the measurement postulate. We explain in Sec.1.5 how this observable can be measured experimentally very easily with a homodyne detector. The RHS of Eq.(1.3.18) is the Radon transform of the Wigner function. Eq.(1.3.18) is the central equation of Chap.?? and provides a way with optical homodyne detection to perform *quantum tomography*, which is the reconstruction of the quantum state through its Wigner function $W(q,p)$ from angular resolved experimental measures of $\langle q|U_\theta \hat{\rho} U_\theta^\dagger|q\rangle$.

Correspondence rules

Since Eq.(1.3.1) defines a linear bijection between $\hat{\rho}$ and $W(q,p)$, any operation which can be described with the former density matrix can be described with the latter Wigner function. Here, we review the most useful links between the operator formalism and Wigner function formalism. First of all, for any two operators $\hat{A}$ and $\hat{B}$, we have the overlap formula or correspondence between the two descriptions

$$\text{tr}\left(\hat{A}\hat{B}\right) = 2\pi \int dq dp W^A(q,p) W^B(q,p), \tag{1.3.19}$$

where $W^A(q,p)$ is defined according to Eq.(1.3.1) with $\hat{\rho} \to \hat{A}$, weither A is Hermitian or not. More generally, a partial trace operation of $\hat{\rho}$ on mode $(\hat{q}_i, \hat{p}_i)$ is expressed on W as an integration over $\mathbb{R}^2$ on the phase space variables (q_i, p_i). Furthermore, an operator correspondence can be established between $\hat{\rho}$ and many phase-space representation of $\hat{\rho}$ [38]. We will only use these correspondence rules together with the Wigner function $W(q,p)$

$$\hat{a}\hat{\rho} \longrightarrow \left(\alpha + \frac{1}{2}\partial_{\alpha^*}\right) W(\alpha, \alpha^*), \quad \hat{\rho}\hat{a} \longrightarrow \left(\alpha - \frac{1}{2}\partial_{\alpha^*}\right) W(\alpha, \alpha^*),$$

$$\hat{a}^\dagger\hat{\rho} \longrightarrow \left(\alpha^* - \frac{1}{2}\partial_{\alpha}\right) W(\alpha, \alpha^*), \quad \hat{\rho}\hat{a}^\dagger \longrightarrow \left(\alpha^* + \frac{1}{2}\partial_{\alpha}\right) W(\alpha, \alpha^*), \tag{1.3.20}$$

with $\alpha = (q + ip)/\sqrt{2}$. Examples of the practical use of Eqs.(1.3.20) are presented in Secs.1.3.4.

Properties

We list in this paragraph the main properties of the Wigner function which are direct consequences of the definition (1.3.1). First, the Wigner function is a normed and bounded function

$$\int dq dp W(p,q) = 1, \text{ and } |W(q,p)| \leq 1/\pi. \tag{1.3.21}$$

From Eq.1.3.19 we deduce the expression of the mean value of an operator $\hat{A}$ as

$$\left\langle \hat{A} \right\rangle = 2\pi \int dq dp W(q,p) W^A(q,p). \tag{1.3.22}$$

The expression of the inner product between two vectors $|\psi_1\rangle$ and $|\psi_2\rangle$ is

$$|\langle\psi_1|\psi_2\rangle|^2 = 2\pi \int dq dp W^1(q,p) W^2(q,p). \tag{1.3.23}$$

The purity of a quantum state is given by

$$\text{tr}(\hat{\rho}^2) = 2\pi \int dq dp W(q,p)^2. \qquad (1.3.24)$$

It is interesting to notice that there is no widely accepted definition of the entropy based on the Wigner function. The von Neumann entropy $S = -\text{tr}[\hat{\rho}\ln\hat{\rho}]$ has no simple expression with $W(q,p)$. Other entropy measures can be defined directly with W, however, none of them seems to have better properties and prevail over the other for applications to the theory of quantum information processing. The consensus at the moment among theorists is to say that this is a mathematical consequence of the infinite-dimensional nature of $\mathcal{H}$ for quantum harmonic oscillators.

1.3.2   The characteristic function

The two-dimensional Fourier transform $\chi(u,v)$ of the Wigner function $W(x,p)$ defined by

$$\chi(u,v) = \int\int dx dp W(x,p) e^{-ivx+iup}, \qquad (1.3.25)$$

is called the *characteristic* function. The inverse transform is given by

$$W(x,p) = \frac{1}{4\pi^2}\int\int du dv \chi(u,v) e^{+ivx-iup}. \qquad (1.3.26)$$

With this particular choise of Fourier norm and sign, $\chi(u,v)$ is equal to the Weyl function, which is defined as the mean value of the displacement operator $\hat{D}_\alpha^\dagger$ with $\alpha = (u+iv)/\sqrt{2}$

$$\chi(u,v) = \left\langle \hat{D}_\alpha^\dagger \right\rangle = \text{tr}\left(\hat{\rho}\, e^{-iv\hat{q}+iu\hat{p}} \right). \qquad (1.3.27)$$

The inverse transform of Eq.(1.3.27) is called the Weyl's expansion of the density matrix and is written

$$\hat{\rho} = \int d^2\alpha \hat{D}_\alpha^\dagger \chi(\alpha). \qquad (1.3.28)$$

As we will see in Chap.**??**, the Weyl function has important properties for quantum tomography. Also, Eqs.(1.3.25) and (1.3.28) together with the definition of the Wigner function in Eq.(1.3.1) close the loop of quantum states representations.

1.3.3   Other phase-space representations

The next two most common phase-space representations of $\hat{\rho}$ after the Wigner function are the Husimi $Q(\alpha)$ and Glauber $P(\alpha)$ representations, with $\alpha \in \mathbb{C}$. The Husimi $Q(\alpha)$ function is a true probability distribution defined as

$$Q(\alpha) = \langle\alpha|\hat{\rho}|\alpha\rangle, \qquad (1.3.29)$$

with $|\alpha\rangle$ a coherent state of amplitude α. $Q(\alpha)$ can be directly measured with a joint homodyne measurement of $\hat{x}$ and $\hat{p}$[26]. The Glauber $P(\alpha)$ function is the counterpart of $Q(\alpha)$ in the sense that it describes $\hat{\rho}$ in the coherent state basis $\{|\alpha\rangle\}$ while $Q(\alpha)$ describes measurements of $\hat{\rho}$ in the same basis. $P(\alpha)$ is defined as the distribution which verifies

$$\hat{\rho} = \int d^2\alpha P(\alpha)|\alpha\rangle\langle\alpha|. \qquad (1.3.30)$$

$P(\alpha)$ is not always a regular function and it exists mathematically only if it is permitted to be a sufficiently singular generalized function. Therefore, it is much harder to manipulate it and

impossible to measure in the general case. Q and P can be used to express respectively anti-normally and normally ordered products of creation and destruction operators

$$\left\langle (\hat{a})^n (\hat{a}^\dagger)^m \right\rangle = \int d^2\alpha Q(\alpha)\alpha^n(\alpha^*)^m, \tag{1.3.31}$$

$$\left\langle (\hat{a}^\dagger)^m (\hat{a})^n \right\rangle = \int d^2\alpha P(\alpha)\alpha^n(\alpha^*)^m. \tag{1.3.32}$$

We will not directly use Q or P in the following chapters, however, it is interesting to emphasize the connection between W, Q and P, which is especially useful to understand the effect on fragile non-Gaussian states of Gaussian decoherence processes such as amplitude dumping or teleportation as we do in Sec.1.3.4 for instance. Similar to Eq.(1.3.25), we define χ_Q and χ_P the 2-dimensional Fourier transforms of Q and P by

$$\chi_Q(\lambda) = \int d^2\alpha Q(\alpha)e^{\lambda^*\alpha - \lambda\alpha^*}, \quad \text{and} \quad \chi_P(\lambda) = \int d^2\alpha P(\alpha)e^{\lambda^*\alpha - \lambda\alpha^*}. \tag{1.3.33}$$

Also similar to Eq.(1.3.27), χ_Q and χ_P can be expressed as expectation values of products of $\exp[-i\alpha\hat{a}^\dagger]$ and $\exp[-i\alpha^*\hat{a}]$ factors:

$$\chi_Q(\lambda) = \left\langle \exp[-i\alpha^*\hat{a}] \exp[-i\alpha\hat{a}^\dagger] \right\rangle, \quad \text{and} \quad \chi_P(\lambda) = \left\langle \exp[-i\alpha\hat{a}^\dagger] \exp[-i\alpha^*\hat{a}] \right\rangle. \tag{1.3.34}$$

With the Baker-Hausdorff formula of Eq.(1.2.24), it is easy to relate the three characteristic functions χ, χ_Q and χ_P of Eqs.(1.3.27) and (1.3.34) together. If we define a generalized characteristic function $\chi(u, v, s)$ parametrized by a real number s in $[-1, +1]$ by

$$\chi(u, v, s) = \chi(u, v)e^{s(u^2+v^2)/4}, \tag{1.3.35}$$

we observe that

$$\chi(\lambda, -1) = \chi_Q(\lambda), \quad \chi(\lambda, 0) = \chi(\lambda), \quad \text{and} \quad \chi(\lambda, +1) = \chi_P(\lambda). \tag{1.3.36}$$

Taking the Fourier transform of Eq.(1.3.35), we obtain the definition of a generalized Wigner function $W(q, p, s)$, where $W(q, p, s)$ can be expressed from $W(q, p, s')$ for $s \leq s'$ by

$$W(q, p, s) = \frac{1}{\pi(s - s')} \int \int dq' dp' W(q', p', s')e^{\left((q-q')^2+(p-p')^2\right)/(s-s')} \tag{1.3.37}$$

We immediately notice that the previously introduced phase-space representations W, Q and P are only special cases of this new generalized Wigner function $W(q, p, s)$:

$$Q(q, p) = W(q, p, -1) \qquad W(q, p) = W(q, p, 0) \qquad P(q, p) = W(q, p, +1) \tag{1.3.38}$$

We also notice that Eq.(1.3.37) in the case $s' = 0$ and $-1 \leq s \leq 0$ can be seen as a convolution of the original Wigner function W with a normalized Gaussian G_σ of standard deviation σ

$$W(q, p, s) = W(q, p) \circ G_\sigma = W(q', p', -2\sigma^2), \tag{1.3.39}$$

with $\sigma = \sqrt{|s|/2}$. If we remember that Q is a true probability distribution and that therefore $Q(\alpha) \geq 0$ for all α, then for any negative Wigner function W, a convolution of W with a Gaussian of standard deviation σ larger than $1/\sqrt{2}$ will always lead to a positive Wigner function according to Eq.(1.3.39). In other words, if we say that a non-classical quantum state has necessary a negative Wigner function, that state can suffer at most losses equivalent to a Gaussian convolution with $\sigma \leq 1/\sqrt{2}$ and still keep a negative Wigner function. This is only a necessary criteria and there exists Wigner functions of mixed states whose negativity will disapear before the $1/\sqrt{2}$ threshold. In Chap.**??**, we apply Eq.(1.3.39) to the teleportation protocol to prove the $3dB$ threshold on non-classical states teleportation.

1.3.4   Linear absorption

Phase-space formulation

In the quantum models of the experimental generated and teleported quantum states developed in Chaps.**??** and **??**, we recurrently use the model of beam-splitters losses introduced in Sec.1.2.7. Here, we show how to adapt Eq.(1.2.53) to the Wigner formalism. First, if $\hat{\rho}$ and $\hat{\rho}'$ are the density matrices of the quantum state respectively before and after losses, using Eq.(1.3.30) we define the Glauber functions $P(\alpha)$ and $P'(\alpha)$ of these two density matrices by

$$\hat{\rho} = \int d^2\alpha P(\alpha)|\alpha\rangle\langle\alpha|, \quad \text{and} \quad \hat{\rho}' = \int d^2\alpha P'(\alpha)|\alpha\rangle\langle\alpha|. \tag{1.3.40}$$

As in Sec.1.2.7, we only assume that the model of linear amplitude dumping is equivalent to the transformation $|\alpha\rangle \to |\sqrt{\eta}\alpha\rangle$. Therefore, $\hat{\rho}'$ can be expressed with $P(\alpha)$

$$\hat{\rho}' = \int d^2\alpha P(\alpha)|\sqrt{\eta}\alpha\rangle\langle\sqrt{\eta}\alpha|, \tag{1.3.41}$$

and a straightforward change of variable proves that $P'(\alpha) = P(\alpha/\sqrt{\eta})/\eta$. Equivalently, we can write this relation with the generalized characteristic and Wigner functions as

$$\chi'(u, v, +1) = \chi(\sqrt{\eta}q, \sqrt{\eta}p, +1), \tag{1.3.42}$$

$$W'(q, p, +1) = \frac{1}{\eta}W(q/\sqrt{\eta}, p/\sqrt{\eta}, +1). \tag{1.3.43}$$

Applying Eq.(1.3.35) on both sides of Eq.(1.3.42), we obtain

$$\chi'(u, v, 0) = \chi(\sqrt{\eta}q, \sqrt{\eta}p, 1 - 1/\eta). \tag{1.3.44}$$

Coming back to the generalized Wigner formalism, Eq.(1.3.44) becomes

$$W(u, v, 0) = \frac{1}{\eta}W(q/\sqrt{\eta}, p/\sqrt{\eta}, 1 - 1/\eta), \tag{1.3.45}$$

which translates with Eq.(1.3.37) into the convolution

$$W'(q, p) = \frac{1}{\eta}\frac{1}{2\pi\lambda^2}\int\int dq'dp'W(q', p')e^{-((q/\sqrt{\eta}-q')^2+(p/\sqrt{\eta}-p')^2)/2\lambda^2}, \tag{1.3.46}$$

with $\lambda = \sqrt{(1-\eta)/2\eta}$. In summary, the beam-splitter model of linear amplitude dumping has for the Wigner function the equivalent formula

$$W(q, p) \overset{\text{losses}}{\longrightarrow} W'(q, p) = \frac{1}{\eta}\left(W \circ G_\lambda\right)\left(\frac{q}{\sqrt{\eta}}, \frac{p}{\sqrt{\eta}}\right). \tag{1.3.47}$$

Omitting the rescaling of phase space, if we apply Eq.(1.3.39) to this model, we find that the strongest amplitude losses η a non-classical state can suffer and still be a non-classical state, in the sense of negativity of the Wigner function, is given by

$$\lambda = \sqrt{(1-\eta)/2\eta} \leq 1/\sqrt{2}, \tag{1.3.48}$$

which gives $\eta \geq 1/2$. Finally, it can be easily proven with Eq.(1.3.46) that two linear amplitude dumping process in a row with amplitude losses coefficients η_1 and η_2 are equivalent to a single process with coefficient $\eta' = \eta_1\eta_2$.
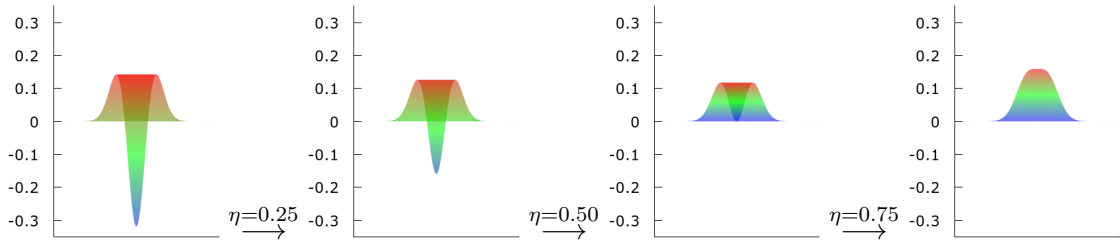
Figure 1.9: Attenuation of the Wigner function of a single photon state through a beam-splitter. From left to right, η equals successively 0, 0.25, 0.5 and finally 0.75.

Master equation

We now have two expressions, one in the photon number basis and one in phase-space, of the same linear amplitude dumping model. To put things in perspective, it is interesting to link Eq.(1.3.47) with the equivalent master equation formulation on $\hat{\rho}$, as was done for example in [46]. First we prove that Eq.(1.3.47) is equivalent to a differential equation. Let's introduce a fictitious time variable t and write $W(q,p) = W(q,p;t_0 = 0)$, $W'(q,p) = W(q,p;t_1 = t)$. We assume that the linear amplitude dumping is equivalent to a continuous dumping process between $t_0 = 0$ and $t_1 = t$ and write $\sqrt{\eta} \to \sqrt{\eta(t)} = \exp[-\gamma t]$ with γ a decay rate constant in Hertz. Eq.(1.3.46) is rewritten

$$W(q,p;t) = \frac{1}{\pi(1 - e^{-2\kappa t})} \int\int dq' dp' W(q,p;0) \exp\left[-\frac{(q - e^{-\kappa t}q')^2 + (p - e^{-\kappa t}p')^2}{1 - e^{-2\kappa t}} \right]. \tag{1.3.49}$$

If we calculate the total time derivative $dW(q,p;t)/dt$ and partial spatial derivatives $\partial_q(W(q,p;t))$ and $\partial_p(W(q,p;t))$, we notice that the ersatz of Eq.(1.3.49) satisfies the differential equation

$$\frac{d}{dt}W(x,p;t) = \gamma\left(\partial_x x + \partial_p p + \frac{1}{4}(\partial_x)^2 + \frac{1}{4}(\partial_p)^2 \right) W(x,p;t). \tag{1.3.50}$$

With the correspondence rules of Eqs.(1.3.20), we immediately obtain the following master equation for $\hat{\rho}$

$$\frac{d}{dt}\hat{\rho}(t) = \gamma\left(2\hat{a}\hat{\rho}\hat{a}^\dagger - \hat{a}^\dagger\hat{a}\hat{\rho} - \hat{\rho}\hat{a}^\dagger\hat{a} \right), \tag{1.3.51}$$

written in the Linblad form as

$$\frac{d}{dt}\hat{\rho}(t) = L[\hat{\rho}(t)] \quad \text{with} \quad L[\hat{\rho}] = \gamma\left([\hat{a}, \hat{\rho}\hat{a}^\dagger] - [\hat{a}^\dagger, \hat{a}\hat{\rho}] \right). \tag{1.3.52}$$

This is the most simple possible form of the Linblad formulation of the master equation. As is explained in Chap.**??**, this model is not equivalent to the damped quantum harmonic oscillator connected to a heat bath at temperature $T \neq 0$. Rather, the master equation (1.3.51) describes a density matrix which will always relax back to the vacuum state $|0\rangle\langle 0|$ as we can notice when solving Eq.(1.3.51) for $d\hat{\rho}/dt = 0$. It therefore describes a perfect relaxation to the ground state of the oscillator at $T = 0$.

1.3.5 Gaussian formalism

Many usual states of quantum optics, such as coherent and squeezed states, have exactly Gaussian shaped Wigner functions and can therefore be described with very few parameters: namely $\langle \hat{q}^2 \rangle$,

$\langle \hat{p}^2 \rangle$ and $\langle \hat{q}\hat{p} \rangle$. It is possible to have a systematic description of these states through their Gaussian correlation matrix Γ defined by

$$\Gamma = \frac{1}{2} \begin{pmatrix} \langle \hat{q}^2 \rangle & \langle \hat{q}\hat{p} \rangle \\ \langle \hat{q}\hat{p} \rangle & \langle \hat{p}^2 \rangle \end{pmatrix}. \tag{1.3.53}$$

The Wigner function of such states can be written using only Γ

$$W(q,p) = \frac{1}{\pi^{\dim} \det(\Gamma)} \exp\left[-\vec{\Phi}^T \, \Gamma^{-1} \, \vec{\Phi} \right], \text{ with } \vec{\Phi} = \begin{pmatrix} q \\ p \end{pmatrix}. \tag{1.3.54}$$

with dim $= 1$ for a 1-mode Wigner function. Eqs.(1.3.53) and (1.3.54) can be extended to composite systems of more than 1 modes, with $\vec{\Phi} = (q_1, p_1, q_2, p_2, \ldots)$ and $\Gamma = \langle \vec{\Phi}.\vec{\Phi}^T \rangle$. As expected, the Gaussian formalism is extremely useful to express in a compact way Gaussian operations on Gaussian states. In Sec.**??** of Chap.**??**, we use the Gaussian formalism to conveniently express the 2-mode EPR correlations shared between Alice and Bob in the theory of the conditional teleportation protocol.

1.4 Multimode quantum optics

In Sec.1.2, we have seen the monomode description of quantum optics, implicitly based on the study of a single quantum harmonic oscillator. Although the physics of monomode quantum optics is already rich, it is almost always irrelevant to actual experimental setups since a pure momomode description assumes at the very least stationary light beams in every respect. Furthermore, a monomode description also ignores all the possible complex spectral properties of non-linear optical phenomena inside crystals for example. In this section, we expand the momonode picture of Sec.1.2 to a multimode quantum description of light. This multimode description proves to be especially important in Chaps.**??** and **??** to develop relevant models of experimentally generated and manipulated quantum states. An interesting reference on the subject and one of the only textbook with a detailed study of multimode quantum optics is [31].

1.4.1 Time and frequency domains

By necessity, almost all multimode analysis have to be conducted in the Heisenberg picture. We start our multimode analysis in this paragraph with the introduction of annihilation and creation operators at different times and frequencies, in the Heisenberg picture.

Annihilation and creation operators

The quantum representation of time-dependent light beam and complex spectral properties requires to extend the basic annihilation $\hat{a}$ and creation $\hat{a}^\dagger$ operators to every plane wave of frequency ω

$$\hat{a} \longrightarrow \hat{a}(\omega) = \hat{a}_\omega, \quad \text{and} \quad \hat{a}^\dagger \longrightarrow \hat{a}^\dagger(\omega) = \hat{a}_\omega^\dagger, \tag{1.4.1}$$

Implicitly, for every frequency mode ω, there is an associated Hamiltonian operator $\hat{H}_\omega = \omega(\hat{a}_\omega^\dagger \hat{a}_\omega + 1/2)$. Since all these Hamiltonians are independent quantum modes, the commutators between $\hat{a}(\omega)$ and $\hat{a}^\dagger(\omega')$ is

$$\left[\hat{a}(\omega), \hat{a}^\dagger(\omega') \right] = \delta(\omega - \omega'). \tag{1.4.2}$$

We define $\hat{a}(t)$ and $\hat{a}^\dagger(t)$ in the time domain with the Fourier transform pairs

$$\hat{a}(t) = \frac{1}{\sqrt{2\pi}} \int d\omega \hat{a}(\omega) e^{-i\omega t}, \qquad (1.4.3)$$

$$\hat{a}(\omega) = \frac{1}{\sqrt{2\pi}} \int dt \hat{a}(t) e^{+i\omega t}, \qquad (1.4.4)$$

$$\qquad (1.4.5)$$

with the commutator $[\hat{a}(t), \hat{a}^\dagger(t')] = \delta(t - t')$. We want to emphasize that these different basis in time or frequency domains only correspond to different decomposition of the Maxwell's equations in Eqs.(1.2.1). Therefore, the multimode character of light is not in any way a quantum property of it, but only a consequence of the dynamics of the Maxwell's equations. In other words, the multimode description of light in quantum optics is simply a choice of a specific point of view and a specific basis to decompose the physical system under study. In the next section, we see how we can adopt a wave-packets basis for multimode quantum optics, an approach especially fruitful to model the non-classical non-Gaussian states generated with photon subtraction. In most cases we are interested in a narrow band of frequency $[-\Delta\omega, +\Delta\omega]$ around the laser central carrier frequency ω_0. In this situation we will often use sideband mode operators at frequency Ω, written in capital letters $\hat{A}$ and $\hat{A}^\dagger$ and defined as

$$\hat{A}_\Omega = \hat{a}_{\omega_0 + \Omega}, \quad \text{and} \quad \hat{A}_t = \hat{a}_t e^{i\omega_0 t}. \qquad (1.4.6)$$

Finally, we write down the total photon number operator over the frequency band $[-\Delta\omega, +\Delta\omega]$ as

$$\hat{n} = \int_{\omega_0 - \Delta\omega}^{\omega_0 + \Delta\omega} d\omega \hat{a}^\dagger(\omega) \hat{a}(\omega). \qquad (1.4.7)$$

The total energy E is written

$$E = \int_{\omega_0 - \Delta\omega}^{\omega_0 + \Delta\omega} d\omega \omega \hat{a}^\dagger(\omega) \hat{a}(\omega), \qquad (1.4.8)$$

with $\hbar = 1$. Usually, we can assume the narrow band approximation $2\Delta\omega << \omega_0$ to be valid and factorise the ω factor outside of the integral in Eq.(1.4.8), which yields for the instantaneous energy $E(t)$ at time t the simple expression $E(t) \propto \hat{n}(t) = \hat{a}^\dagger(t)\hat{a}(t)$, a relation we use in Sec.1.5.2 to model a broadband homodyne detector.

1.4.2 Wave-packet states

We define a quantum mode $(\hat{a}_f, \hat{a}_f^\dagger)$ through the transformation

$$\hat{a}_f = \int d\omega \tilde{f}^*(\omega) \hat{a}(\omega) = \int d\omega f(t)^* \hat{a}(t), \qquad (1.4.9)$$

$$\hat{a}_f^\dagger = \int d\omega \tilde{f}(\omega) \hat{a}^\dagger(\omega) = \int d\omega f(t) \hat{a}^\dagger(t). \qquad (1.4.10)$$

where $\tilde{f}(\omega)$ is the Fourier transform of $f(t)$ and where $f(t)$ verifies $\int |f(t)|^2 dt = 1$ so that $[\hat{a}_f, \hat{a}_f^\dagger] = 1$. The commutator of $\hat{a}_\omega$ with $\hat{a}_f^\dagger$ is given by

$$\left[\hat{a}(\omega), \left(\hat{a}_f^\dagger\right)^n\right] = n\tilde{f}(\omega) \left(\hat{a}_f^\dagger\right)^{n-1}. \qquad (1.4.11)$$

The quantum mode defined by $f(t)$ can be effectively regarded as a wave-packet quantum mode unless $f(t)$ is simply a plane wave $\exp[-i\omega t]$. Such a mode is adequate to describe pulses of light

where the electrical field exactly follows $f(t)$. If we define $(\hat{A}_f, \hat{A}_f^\dagger)$ with the sideband operators $(\hat{A}_\Omega, \hat{A}_\Omega^\dagger)$, then $f(t)$ is the envelop of the electrical field quickly oscillating at the laser central carrier frequency ω_0. Instead of using the time or frequency domains, it is actually possible to define a basis of such wave-packet quantum modes to describe all multimode properties of light. We introduce a set of functions $\{f_n(t)\}$ and define for every n a quantum mode $\hat{a}_n$ by

$$\hat{a}_n = \int dt f_n(t)\hat{a}(t). \tag{1.4.12}$$

To ensure that $[\hat{a}_n, \hat{a}_m^\dagger] = \delta_n^m$ and obtain a valid multimode decomposition of the Maxwell's equations, the set of functions $\{f_n(t)\}$ needs only to verify $\int dt f_n(t) f_m^*(t) = \delta_n^m$ for every n and m. In other words, any set of orthonormal functions $\{f_n(t)\}$ can be used to define a set of independent wave-packet quantum modes describing as many independent quantum harmonic oscillators. The reverse transform of Eq.(1.4.12) is simply

$$\hat{a}(t) = \sum_n f_n^*(t)\hat{a}_n, \tag{1.4.13}$$

which allows to decompose a time domain or frequency domain expression onto a wave-packet modes basis. The closure relation $\sum_n f_n(t) f_n^*(t') = \delta(t - t')$ allows to easily go from Eq.(1.4.12) to Eq.(1.4.13).

One photon pulse

A one photon pulse of light with an electrical field described by $f(t)$ is simply written $|1\rangle_f = \hat{a}_f^\dagger |0\rangle$. In the frequency domain for example, it can really be thought of as a weighted superposition of single photon states over different frequencies

$$|1\rangle_f = \int_{-\infty}^{+\infty} d\omega f(\omega) \left(\hat{a}^\dagger(\omega)|0\rangle \right). \tag{1.4.14}$$

This is in practice the most faithful way to describe a freely propagating single photon quantum state of light in most experiments, where $f(\omega)$ would account for the spectral characteristics of the particle source.

Coherent pulse

It is also possible to define a generalized coherent state $|\alpha\rangle_f$, where α is any complex number, as

$$|\alpha\rangle_f = \exp\left[\alpha \hat{a}_f^\dagger - \alpha^* \hat{a}_f\right]. \tag{1.4.15}$$

$|\alpha\rangle_f$ is an eigenstate of $\hat{a}_f$ with eigenvalue α. It is also an eigenstate of $\hat{a}(t)$ or $\hat{a}(\omega)$ with the slightly different eigenvalue relations

$$\hat{a}(\omega)|\alpha\rangle = \alpha \tilde{f}(\omega)|\alpha_f\rangle, \quad \text{and} \quad \hat{a}(t)|\alpha\rangle = \alpha f(t)|\alpha_f\rangle. \tag{1.4.16}$$

Two photons pulse

Although we can define photon number states $|2\rangle_f$, $|3\rangle_f$, ... in a way similar to Eq.(1.4.14), a two photons pulse can show much more complex spectral properties, and especially entanglement

between different spectral components. It is valid in general to write any two-photon state $|1+1\rangle$ in the form

$$|1+1\rangle = \frac{1}{\sqrt{2}} \int_{-\infty}^{+\infty} d\omega \int_{-\infty}^{+\infty} d\omega' g(\omega, \omega') \hat{a}^\dagger(\omega) \hat{a}^\dagger(\omega') |0\rangle, \qquad (1.4.17)$$

with the only necessary restrictions being that $\int d\omega \int d\omega' |g(\omega, \omega')|^2 = 1$ for normalization of $|1+1\rangle$ and that $g(\omega, \omega') = g(\omega', \omega)$ because photons are bosons. To convince ourselves that $|1+1\rangle$ contains 2 photons, we compute $\langle 1+1|\hat{n}|1+1\rangle$ where $\hat{n}$ is given by Eq.(1.4.7) and obtain 2. Only if $g(\omega, \omega') = f(\omega)f(\omega')$ would we have the 2 photons number state $|2\rangle_f$ in the wavepacket $f(t)$. In the most general case, $g(\omega, \omega')$ describes frequency correlations between these two photons, and unless $g(\omega, \omega')$ can be factorized between both frequency variables, these photons are indeed entangled in their spectral components. Similar to Eq.(1.4.17), we can also define a two-photon pulses in two different spatial modes $\hat{a}$ and $\hat{b}$ by

$$|1_a, 1_b\rangle = \frac{1}{\sqrt{2}} \int_{-\infty}^{+\infty} d\omega \int_{-\infty}^{+\infty} d\omega' h(\omega, \omega') \hat{a}^\dagger(\omega) \hat{b}^\dagger(\omega') |0\rangle. \qquad (1.4.18)$$

Here, the symmetry of $h(\omega, \omega')$ is not required and only $\int d\omega \int d\omega' |h(\omega, \omega')|^2 = 1$ is necessary. The essential experimental difference between $|1+1\rangle$ and $|1_a, 1_b\rangle$ is the possibility to always being able to seperate $|1_a, 1_b\rangle$ into two by physically seperating modes a and b.

1.4.3 Broadband squeezing

While Eq.(1.4.17) is useful to describe broadband squeezed vacuum states generated from the central degenerate mode of an optical parametric oscillator (OPO), Eq.(1.4.18) is useful do describe correlated photons generate by an OPO in symmetric resonant modes. To understand the multimode properties of the photon subtraction protocol, we are particulary interested in Eq.(1.4.17) which we use to define a broadband squeezing operator.

The first squeezing experiments were conducted both in the pulsed and the continuous regimes in the mid and late eigthies [15, 16, 17]. In the continuous wave regime where it is difficult to obtain strong non-linear effects with low amplitude electrical field, OPO plays a central role for the generation of highly squeezed quantum states. Although continuous wave regime setups are much more complicated, these OPO setups can achieve much higher level of squeezing and purer quantum states [42, 50, 57]. Currently 12.7 dB is the highest level of squeezing using a monolithic cavity configuration based around a periodically poled potassium titanyl phosphate crystal as reported in [62]. In this letter it is shown how this strongly squeezed light has been experimentally used to improve the noise floor of a Sagnac interferometer. It was noted early on that squeezed light emitted from OPO had complex spectral properties[13]. These spectral properties have been studied by many, both theoretically[13, 19, 20, 32, 37, 39, 44] and experimentally [35, 53]. We do not derive and get into the full details of the OPO theory, as it has been amply treated in many articles and thesis in the past. Instead, we only summarize the most important results and, more importantly, write the exact multimode squeezing operator necessary in Chap.**??**.

Time and frequency correlation functions

With a careful model of the non-linear interaction Hamiltonian describing the parametric-down conversion process inside the non-linear crystal, and the consideration of the cavity around this crystal, it is possible to derive frequency and time mean correlation functions in the output field annihilation and creation operators. See for example [13, 19, 20] for details. For the degenerate
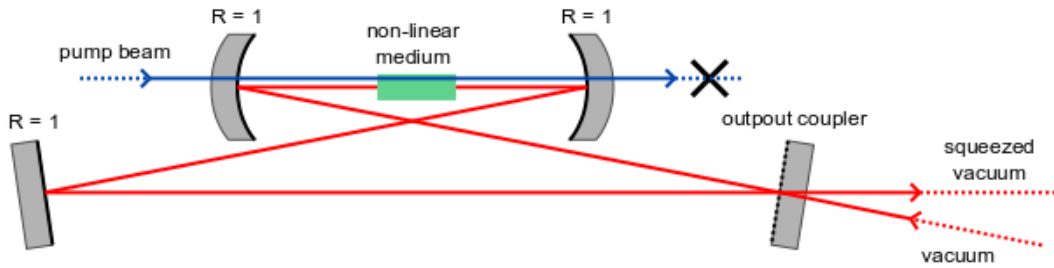
Figure 1.10: Typical bow-tie cavity based optical parametric oscillator.

central mode of an OPO, we have

$$\langle \hat{a}(t)\hat{a}(t')\rangle = \frac{\lambda^2 - \mu^2}{4}\left(\frac{e^{-\mu|t-t'|}}{2\mu} + \frac{e^{-\lambda|t-t'|}}{2\lambda}\right), \tag{1.4.19}$$

$$\langle \hat{a}^\dagger(t)\hat{a}(t')\rangle = \frac{\lambda^2 - \mu^2}{4}\left(\frac{e^{-\mu|t-t'|}}{2\mu} - \frac{e^{-\lambda|t-t'|}}{2\lambda}\right), \tag{1.4.20}$$

where $\lambda = \gamma/2 + \epsilon$ and $\mu = \gamma/2 - \epsilon$, with γ the cavity decay rate, including losses, and ϵ the non-linear gain in the crystal. For a non-degenerate OPO with two output modes $\hat{a}_+$ and $\hat{a}_-$, we have

$$\langle \hat{a}_\pm(t)\hat{a}_\mp(t')\rangle = \frac{\lambda^2 - \mu^2}{4}\left(\frac{e^{-\mu|t-t'|}}{2\mu} + \frac{e^{-\lambda|t-t'|}}{2\lambda}\right), \tag{1.4.21}$$

$$\langle \hat{a}_\pm^\dagger(t)\hat{a}_\pm(t')\rangle = \frac{\lambda^2 - \mu^2}{4}\left(\frac{e^{-\mu|t-t'|}}{2\mu} - \frac{e^{-\lambda|t-t'|}}{2\lambda}\right). \tag{1.4.22}$$

$\hat{a}_+$ and $\hat{a}_-$ can be either two symmetric resonant modes around the central resonant mode of the OPO, or the two polarization central resonant modes of a type II OPO.

Broadband squeezing operator

In practice, Eqs.(1.4.19) and (1.4.21) are not sufficient for our purpose. We would rather express a multimode squeezed vacuum state with the help of an appropriately defined squeezing operator. By combining the definition of the monomode squeezing operator $\hat{S}_s = \exp[s((\hat{a})^2 - (\hat{a}^\dagger)^2)/2]$ in Eq.(1.2.34) and the expression of the two photons pulse state in Eq.(1.4.17), we can obtain such an operator with the substitution

$$\frac{s}{2}\hat{a}^2 \longrightarrow \int d\Omega d\Omega' \frac{g(\omega_0 + \Omega, \omega_0 - \Omega')}{2}\hat{a}(\omega_0 + \Omega)\hat{a}(\omega_0 - \Omega'), \tag{1.4.23}$$

where $g(\omega_0 + \Omega, \omega_0 - \Omega')$ contains all the spectral properties of the parametric down conversion process happening inside the crystal, itself put inside the OPO cavity. Since the OPO is pumped at $2\omega_0$ and the parametric-down conversion process conserves energy, $g(\omega_0 + \Omega, \omega_0 - \Omega')$ can be assumed to have the form $\zeta(\Omega)\delta(\Omega - \Omega')$ or $\zeta_\Omega \delta(\Omega - \Omega')$ with the sideband symmetry relation $\zeta_{+\Omega} = \zeta_{-\Omega}$. We obtain the simplified expression of the broadband squeezing operator as

$$\hat{S} = \exp\left[\int d\Omega \frac{\zeta_\Omega}{2}\left(\hat{A}_{+\Omega}\hat{A}_{-\Omega} - \hat{A}_{+\Omega}^\dagger \hat{A}_{-\Omega}^\dagger\right)\right], \tag{1.4.24}$$

with the sideband notation $\hat{A}_\Omega = \hat{a}(\omega_0 + \Omega)$. With the development rule of Eq.(1.2.35), we can write the effect of $\hat{S}$ on sideband modes $\hat{A}_\Omega$ as the following Bogoliubov transformation

$$\hat{S}^\dagger \hat{A}_\Omega \hat{S} = \cosh(\zeta_\Omega)\hat{A}_\Omega - \sinh(\zeta_\Omega)\hat{A}^\dagger_{-\Omega}, \tag{1.4.25}$$

where the mixing of upper $+\Omega$ and lower $-\Omega$ frequency sidebands is readily apparent. With Eq.(1.4.25) the two frequencies mean correlation functions can be calculated

$$\left\langle \hat{A}^\dagger_\Omega \hat{A}_{\Omega'} \right\rangle = (\sinh \zeta_\Omega)^2 \, \delta(\Omega - \Omega'), \tag{1.4.26}$$

$$\left\langle \hat{A}_\Omega \hat{A}_{\Omega'} \right\rangle = -\sinh(\zeta_\Omega)\cosh(\zeta_\Omega)\,\delta(\Omega + \Omega'). \tag{1.4.27}$$

By identification of Eqs.(1.4.19) and (1.4.26), we can relate the spectral correlation function ζ_Ω to the relevant OPO parameters γ and ϵ.

How different this new multimode squeezing operator is from the monomode formulation of Eq.(1.2.34)? To investigate this question we define a basis of wave-packets mode $\{\hat{A}_n\}$ using the set of real, symmetric and orthonormal functions $\{\phi_n(\omega)\}$ in the same way as in Eq.(1.4.12)

$$\hat{A}_n = \int d\Omega \phi_n(\Omega)\hat{A}_\Omega, \tag{1.4.28}$$

$$\hat{A}_\Omega = \sum_n \phi_n(\Omega)\hat{A}_n. \tag{1.4.29}$$

$$\tag{1.4.30}$$

If $\zeta_\Omega = s$ happens to be a constant function, $\hat{S}$ will be written

$$\hat{S} \overset{\zeta_\Omega = s}{=} \exp\left[\frac{s}{2}\sum_n\left(\left(\hat{A}_n\right)^2 - \left(\hat{A}^\dagger_n\right)^2\right)\right] = \bigotimes_n \exp\left[\frac{s}{2}\left(\left(\hat{A}_n\right)^2 - \left(\hat{A}^\dagger_n\right)^2\right)\right]. \tag{1.4.31}$$

Which is simply a factorized product of independent squeezing operators acting on different wave-packet modes. In this situation, monomode of multimode squeezing operators are the same. However, this is only a limit case or approximation at best, at least because the bandwidth of spectral correlations needs to be cut at some upper frequency point. In the general case, for any function ζ, $\hat{S}$ can be written

$$\hat{S} = \exp\left[\frac{1}{2}\vec{\hat{A}}.\bar{\zeta}.\vec{\hat{A}} - \frac{1}{2}\vec{\hat{A}}^\dagger.\bar{\zeta}.\vec{\hat{A}}^\dagger\right], \tag{1.4.32}$$

where $\vec{\hat{A}}$ is the operator vector $(\hat{A}_0, \hat{A}_1, \ldots)$ and $\bar{\zeta}$ is a matrix whose elements $(\bar{\zeta})_{n,m}$ are

$$\left(\bar{\zeta}\right)_{n,m} = \int d\Omega \zeta_\Omega \phi_n(\Omega)\phi_m(\Omega). \tag{1.4.33}$$

The off-diagonal elements of the matrix $\bar{\zeta}$ describe the entanglement between the different wave-packet modes caused by the spectral correlation function ζ_Ω. With actual experimental parameters of typical OPOs in the weak pumping regime, these off-diagonal terms turn out to be only a fraction of the corresponding diagonal elements. In other words, they are almost invisible in measurements and irrelevant for numerical applications. Actual numerical applications can be found in [61] and [49, 48].

Eqs.(1.4.24) and (1.4.25) contain all the multimode behavior we need to correctly describe experimentally generated photon-subtracted squeezed vacuum states in Chap.**??**. Rather than introducing new tools, in this section we have explained how to combine the existing tools of Sec.1.2 in way a relevant for our purpose. From now on, the multimode description of light is a matter of applying the definitions of this section with care and in the good spatio-temporal basis.

1.5   Detection of ligth

The possibility to build homodyne detectors able to resolve the quantum shotnoise power level with tens of decibels of signal to noise ratio with off-the-shelves components such as PIN photodiodes and operational amplifiers is a blessing for the field of quantum optics. Without easy detection of light and the availaibility of low-noise electronics circuitry, quantum optics experiments would certainly not have known such a rapid development since the invention of the laser. The microscopic details of light absorption by matter is incredibly complex, but these complex phenomenon can be tamed to engineer many different physical detection devices with nice properties that can be described by simple yet efficient models. This field of research is still very active today, with applications in many major industries, such as imaging technologies, digital cameras and video recording, communication and information networks, solar energy, ... Until now, the bread and butter of light detection for quantum optics experiments has always been the PIN photodiode, with silicon and gallium arsenide as the two main semiconductor technologies employed. This is the only device on which we focus our attention in this thesis. However, some new technologies have recently made their appearance with interesting properties for non-linear detector applications in quantum optics [60]. For instance the currently most promising technology is certainly supra-conducting transition edge sensors[28, 33, 55] and super-conducting nanowire single-photon detectors[54, 59].

In this section, we focus on the description of light detection and quantum field measurement. We review the main detection device experimentally used in this thesis, the PIN silicon photodiode, both in its linear and avalanche regimes. Also, we describe models to include detection losses, extra electronic noise, and multimode light detection.

1.5.1   Intensity detection

Intensity detection relies on the direct absorption of light by matter. At the quantum level, an intensity detector will only be able to measure $\hat{n} = \hat{a}^\dagger \hat{a}$ or some derivative of $\hat{n}$, but will not be able to measure linear combination of $\hat{a}$ and $\hat{a}^\dagger$. The previously mentioned supra-conducting detectors have been able to measure and discriminate individually different photon number states of light, therefore achieving partially the measurement operator $|n\rangle\langle n|$. PIN photodiodes are not at that level of precision, but offer other advantages in term of bandwidth, recovery time, and ease of utilisation.

Photodiodes

For circuits design, the photodiode is a diode in parallel with a current source i, also called the *photocurrent*, where i is proportional to the incoming light intensity. From an electrical point of view, a PIN photodiode is nothing else than a simple PIN diode, made with a P-N semiconductor junction and an additional "I" semiconductor layer in the middle. The I layer acts as a pool of charge carriers and accepts carriers from the P and N layers until a threshold is reached and current starts to flow through the junction. This I layer drastically enhances the linearity of the photocurrent with incoming light. The photodiode effect is simply a consequence of the photoelectric effect where incoming photons are converted to charge carriers. PIN photodiodes are blessed with many desirable characteristics. First of all, being made of silicon for infrared light detection, they are quite inexpensive. Also, in the infrared and near-infrared, they can be engineered to reach very high level of light conversion efficiency, a parameter also called quantum efficiency, with many devices above the 95% mark. Their detection bandwidth can reach the gigahertz, at the expense of quantum efficiency. 99% efficient diodes can be run in the tens of megahertz with ease. Their

intrinsic dark current or dark noise, the electrical current generated at room temperature by a photodiode in the absence of incoming light, is also usually much lower than the shotnoise power of light in the vacuum state.

Linear regime

In the linear regime, PIN photiodes are usually connected with a reverse voltage biasing across electrodes. The voltage bias reduces the capacity of the semiconductor layers, therefore increasing the bandwidth dramatically. The bias also induces some additional dark noise, usually in negligible amount. Thanks to the PIN architecture, the photocurrent i shows a very linear response to the incoming light intensity $\hat{n}$ on a dynamic scale of tens of magnitude order. At the quantum level, we can introduce $\hat{i}$ the photocurrent operator which is assumed to be written

$$\hat{i} = g \sum_k \hat{a}_k^\dagger \hat{a}_k, \tag{1.5.1}$$

where g is the gain of the photodiode and k refers to all incident spatial modes illuminating the photodiode active area. In this scenario the classical variable photocurrent i is simply a random variable with a probability distribution $p(i)$ equal to

$$p(i) = \text{tr}\left[\hat{i}\hat{\rho}\right]. \tag{1.5.2}$$

1.5.2 Amplitude detection

With current technology, direct amplitude detection of an electrical field oscillating as fast as light is not easily possible. No electronics circuits can keep with optical frequencies with a sufficiently large bandwidth, although progress in nanotechnologies might allow for such devices in the future. Amplitude detection of light has to be achieved with indirect means, essentially through interferences with light oscillating as fast or faster than the light beam to be measured. In pulse light experiments there is a variety of different interferometric measurement techniques for characterisation of ultra short pulses of light. In the continuous wave regime only one interferometric measurement, the homodyne measurement, is really needed.

Homodyne measurement

An homodyne detector is made of a beam splitter and two photodiodes. The incoming light mode is mixed on the beam-splitter with a *local oscillator* beam. Both output modes are measured by both photodiodes, and the two photocurrents are then subtracted. The homodyne detector operator $\hat{D}$ can be written in the output modes as

$$\hat{D} = g\left(\hat{d}^\dagger \hat{d} - \hat{c}^\dagger \hat{c}\right), \tag{1.5.3}$$

where g is the photodiode conversion gain. We rewrite $\hat{D}$ in the input modes and obtain

$$\hat{D} = grt\left(\hat{a}\hat{b}^\dagger - \hat{a}^\dagger \hat{b}\right), \tag{1.5.4}$$

with r and t being the amplitude reflection and transmission coefficients of the beam splitter. For a balanced homodyne detector, rt is maximal and is equal to $1/2$. The local oscillator is a strong laser beam in a coherent state $|\alpha\rangle$. We project mode $\hat{b}$ onto the coherent state $|\alpha\rangle = |\rho e^{i\theta}\rangle$ and define the homodyne current operator $\hat{i} = \langle\alpha|\hat{D}|\alpha\rangle$

$$\hat{i} = grt\rho\left(\cos\theta\hat{x} + \sin\theta\hat{p}\right) \tag{1.5.5}$$
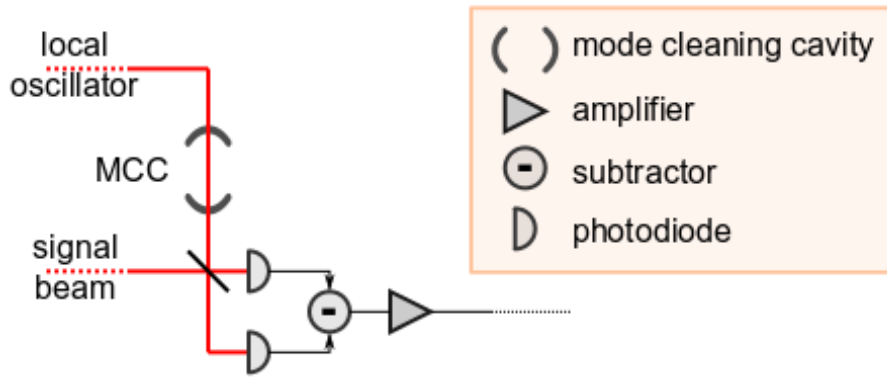
Figure 1.11: Setup for optical homodyne measurement. The mode cleaning cavity helps to enhance the overlap between the spatial modes of the signal and local oscillator.

We notice that by controlling the relative phase θ of the local oscillator relatively to the incoming signal mode, the homodyne current $\hat{i}$ can be adjusted to measure any angle in the quadrature basis. Also, the intensity ρ^2 of the local oscillator can be adjusted to obtain a stronger photocurrent and a higher signal to noise ratio, within the limit of saturation of the photodiode semiconductor layers.

Detection of broadband light

If we want to measure light over a broad spectrum of frequencies, we need to consider the photocurrent operator at every point of time $\hat{i} \to \hat{i}(t)$. We measure $\hat{i}(t)$ over some interval Δt and look at the Fourier transform of the time series $i(t)$. The expression of the homodyne detector operator of the previous paragraph is still valid as long as we consider $\hat{D}$ for every time instant t.

$$\hat{D}(t) = grt \left(\hat{a}_t \hat{b}_t^\dagger - \hat{a}_t^\dagger \hat{b}_t \right). \tag{1.5.6}$$

We assume the inverse of the laser line-width to be smaller than any other time constant involved in the detection. Therefore, the projection of $\hat{b}$ onto $|\alpha\rangle\langle\alpha|$ at time t simply adds a rapidly oscillating complex phase whose power is averaged by the semiconductor layers inside and photodiodes and by the external electrical circuit. We expand the signal mode $\hat{a}(t)$ on an orthonormal basis of wave-packet modes $\{f_n(t)\}$ and obtain for the multimode detector operator $\hat{D}(t)$

$$\hat{D}(t) = grt \sum_n f_n(t) \left(\hat{A}_n \hat{b}_t^\dagger - \hat{A}_n^\dagger \hat{b}_t \right), \tag{1.5.7}$$

and for the homodyne current

$$\hat{i}(t) = grt\rho \sum_n f_n(t) \left(\cos\theta \hat{X}_n - \sin\theta \hat{P}_n \right). \tag{1.5.8}$$

We notice that the homodyne detector probes many different wave-packet modes at the same time in the same measurement. The photocurrent operators is indeed a sum of the different quadrature operators of all these modes, all measured at the same relative phase θ. From now on we assume $\theta = 0$ for simplicity. If we call $|Y\rangle_n$ the eigenvector of the quadrature operator $\hat{X}_n$ with eigenvalue Y, then the eigenvectors of $\hat{i}$ are

$$\bigotimes |Y_m\rangle_m = |\overrightarrow{Y}\rangle, \tag{1.5.9}$$

with eigenvalues

$$\sum_n f_n(t)Y_n. \tag{1.5.10}$$

We define the three vectors $\overrightarrow{f}(t) = (f_0(t), f_1(t), \ldots)$, $\overrightarrow{Y} = (Y_1, Y_2, \ldots)$ and $|\overrightarrow{Y}\rangle = \bigotimes |Y_m\rangle_m$ which we use to express the above eigenvector relation as

$$\hat{i}(t)|\overrightarrow{Y}\rangle = \left(\overrightarrow{f}.\overrightarrow{Y}\right)|\overrightarrow{Y}\rangle \tag{1.5.11}$$

In short, for every time series measurement of $\hat{i}(t)$ over an interval Δt, an eigenvalue $\overrightarrow{Y}$ is randomly observed with the underlying probability distribution $\langle\overrightarrow{Y}|\hat{\rho}|\overrightarrow{Y}\rangle$. Therefore the shotnoise normalized homodyne current $U(t)$ is a random process written

$$U(t) = \left(\overrightarrow{f}.\overrightarrow{Y}\right) = \sum_n f_n(t)Y_n. \tag{1.5.12}$$

If there is no entanglement between the different modes, every values Y_n is an independent random variable with its marginal distribution $p_n(y)$ given by

$$p_n(y) = p\left(Y_n = y\right) = \langle y|\text{tr}\left[\hat{\rho}\right]_{m\neq n}|y\rangle \tag{1.5.13}$$

We see that with projections of the homodyne current $\int dt f_k(t)U(t)$ onto the different wave-packet modes, thanks to the orthogonality of the wave-packet basis $\{f_n(t)\}$, a smart analysis of the photocurrent time series can retrieve and separate every single mode. Furthermore, by combining the different projections $\int dt f_k(t)U(t)$, it is also possible to retrieve entanglement between the different wave-packet modes.

1.5.3 Inneficient homodyne detection

There is no such things as a perfect measurement. In this section we investigate the effect of optical losses, imperfect homodyne visibility, imperfect photodiode conversion efficiency, and electronic noise on the process of homodyne measurement. Since the homodyne measurement is a Gaussian measurement, all these sources of imperfections can be modeled with linear amplitude dumping model of Sec.1.3.4. Therefore, we prove for all these case their equivalence to the beam-splitter model of lineal amplitude losses.

Optical losses and finite quantum efficiency

The effect of any optical losses on the signal mode before the homodyne beam splitter has already been covered in Sec.1.3.4. Losses on the local oscillator beam only reduces its amplitude $|\alpha|^2$. Now, we assume the presence of two beam-splitters with amplitude transmission coefficients $\sqrt{\eta}$ in front of the photodiodes. If we call $\hat{e}$, $\hat{f}$ the auxiliary modes in the vacuum states mixed in at these additional beam-splitters, and $\hat{c}'$, $\hat{d}'$ the output modes incoming into the photodiodes, we can write the effect of these beam-splitters as

$$\left(\hat{d}'^\dagger\hat{d}' - \hat{c}'^\dagger\hat{c}'\right) = \eta\left(\hat{d}^\dagger\hat{d} - \hat{c}^\dagger\hat{c}\right) + (1-\eta)\left(\hat{f}^\dagger\hat{f} - \hat{e}^\dagger\hat{e}\right) + \sqrt{\eta(1-\eta)}\left(\hat{c}^\dagger\hat{e} + \hat{e}^\dagger\hat{c} + \hat{d}^\dagger\hat{f} + \hat{f}^\dagger\hat{d}\right). \tag{1.5.14}$$

The first term of the RHS of Eq. is the expression of the homodyne detector operator $\hat{D}$ from Eq.(1.5.3) without losses. The second term of the RHS of Eq.(1.5.14) has no contribution to the

final photocurrent after modes $\hat{e}$ and $\hat{f}$ are projected onto the vacuum state. The third term of the RHS of Eq.(1.5.14) can be rewritten as

$$\frac{\sqrt{\eta(1-\eta)}}{2}\left(\hat{b}^\dagger(\hat{e}+\hat{f})+\hat{b}(\hat{e}^\dagger+\hat{f}^\dagger)\right), \tag{1.5.15}$$

neglecting terms in $\hat{a}$. Keeping only contributing terms of Eq.(1.5.14), the imperfect detector operator $\hat{D}_\eta$ can be written as

$$\hat{D}_\eta \;\propto\; \sqrt{\eta}\left(\hat{b}^\dagger\hat{a}+\hat{a}^\dagger\hat{b}\right)+\frac{\sqrt{1-\eta}}{2}\left(\hat{b}^\dagger(\hat{e}+\hat{f})+\hat{b}(\hat{e}^\dagger+\hat{f}^\dagger)\right) \tag{1.5.16}$$

$$\propto\; \hat{b}^\dagger\left(\sqrt{\eta}\hat{a}+\frac{\sqrt{1-\eta}}{2}(\hat{e}+\hat{f})\right)+\hat{b}\left(\sqrt{\eta}\hat{a}^\dagger+\frac{\sqrt{1-\eta}}{2}(\hat{e}^\dagger+\hat{f}^\dagger)\right). \tag{1.5.17}$$

The effect of these beam splitters is equivalent to a single beam-splitter with amplitude transmission coefficient $\sqrt{\eta}$ placed on the signal beam before the homodyne detector. In essence, we have only shown that the additional beam-splitters can be commuted outside of the homodyne detection. Eq.(1.5.17) formally proves that any optical losses inside the homodyne detector can be described with the model of linear amplitude dumping of Sec.1.3.4 and a single transmission efficiency coefficient.

Imperfect quantum efficiency

The effect of imperfect quantum efficiency of photodiodes is exactly similar to optical losses in front of the photodiodes. This effect can be modeled in the same way as in the previous paragraph, and accounted for with a single parameter.

Imperfect spatial overlap

In the homodyne measurement technique, the local oscillator defines which spatial mode is being measured. In effect, only the photon flux of the signal beam in the exact same overlapping mode as the local oscillator is measured by the homodyne detector. In other words, an imperfect mode matching or imperfect overlap between the local oscillator and signal beams leads to a loss of information through the photons of the signal beam not interfering with the local oscillator. As with the previous loss mechanisms, a situation of imperfect spatial overlap can be fully described by the same linear amplitude dumping model with a single efficiency coefficient usually called the homodyne detector *visibility*. Details about the analysis of this effect can be found for example in [26].

Electronic noise

Finally we study the effect of additional electrical noise in the homodyne detector circuitry. A similar analysis can be found in [45]. We assume that we use homodyne detection to record the statistics of an unknown quantum state and use the homodyne current to perform tomographic reconstruction of the Wigner function (see Chap.**??** for details). The homodyne current random variable i is crippled by an unknown Gaussian noise that cannot be distinguished from the information of the quantum state. We know from Eq.(1.3.18) that the Wigner function is linked to the probability distribution of the photocurrent by the Radon transform:

$$p(x,\theta)=\mathcal{R}\left(W\right)\;=\;\iint_{\mathbb{R}^2}W(q,p)\delta(x-q\cos\theta-p\sin\theta)dqdp, \tag{1.5.18}$$

$$=\;\int_{-\infty}^{+\infty}W(x\cos\theta-p\sin\theta,x\sin\theta+p\cos\theta)dp. \tag{1.5.19}$$

The difficulty of the analysis is to understand how a pure classical source of noise affects the purity of the quantum state being measured. In our analysis we will use the four following results:

1. If a random variable X has a distribution $p(X = x) = p_X(x)$ then the random variable aX has for distribution $p(aX = x) = p_X(x/a)/a$. In the case of a Gaussian distribution $G_\sigma(x)$ of standard deviation σ, we obtain the distribution $G_{a\sigma}(x)$.

$$p(aX = x) = \frac{1}{a}p(X = x/a). \tag{1.5.20}$$

2. If X and Y are two independent random variables with distribution $p_X(x) = p(X = x)$ and $p_Y(x) = p(Y = x)$, then the random variables $Z = X + Y$ has for distribution $p_X \circ p_Y$. In the case of two Gaussian distributions of standard deviations σ and σ' we obtain a Gaussian distribution of standard deviation $\sqrt{\sigma^2 + \sigma'^2}$.

$$p_{X+Y}(x) = (p_X \circ p_Y)(x). \tag{1.5.21}$$

3. If W_X and W_Y are two Wigner functions whose Radon transforms are the marginal distributions p_X and p_Y, then the Wigner function $W_Z = W_X \circ \circ W_Y$ has for Radon transform $p_X \circ p_Y$, where $\circ\circ$ denotes a 2-dimensional convolution:

$$\mathcal{R}(W_X \circ \circ W_Y)(x, \theta) = (\mathcal{R}(W_X) \circ \mathcal{R}(W_Y))(x, \theta). \tag{1.5.22}$$

4. If $p(x, \theta)$ is the Radon transform of $W(q, p)$, then the Radon transform of $W(q/a, p/a)$ is $ap(x/a, \theta)$:

$$\frac{1}{a}\mathcal{R}(W(q/a, p/a))(x, \theta) = \mathcal{R}(W(q, p))(x/a, \theta). \tag{1.5.23}$$

Armed with this four lemmes, we assume that the raw homodyne current U is the sum of two independent random variables X and Y

$$U = g(X + Y), \tag{1.5.24}$$

with g the detection gain. X is distributed according to $p(x, \theta)$ the distribution of the original quantum state we want to measure. Y is an additional Gaussian noise of standard deviation $\sigma = \epsilon/\sqrt{2}$. Now let's assume that we calibrate the homodyne detection with a measure of the variance of the vacuum $|0\rangle$. The homodyne current is now the random variable V

$$V = g(X_0 + Y), \tag{1.5.25}$$

with X_0 having for distribution a Gaussian of standard deviation $1/\sqrt{2}$. From above results 1) and 2), V will be a Gaussian of standard deviation $\sigma_V = g\sqrt{1 + \epsilon^2}/\sqrt{2}$. We now renormalize U to the measured vacuum noise standard deviation $\sqrt{2}\sigma_V$ and obtain

$$U \to U' = \frac{1}{\sqrt{2}\sigma_V}U = \frac{1}{\sqrt{(1 + \epsilon^2)}}(X + Y). \tag{1.5.26}$$

According to results 1) and 2), the probability distribution of U' is

$$p(U' = x) = \sqrt{1 + \epsilon^2}\left(p_X \circ G_{\epsilon/\sqrt{2}}\right)(\sqrt{1 + \epsilon^2}x), \tag{1.5.27}$$

whose Wigner function $W_{U'}$ can be expressed with results 3) and 4) as

$$W_{U'}(q, p) = (1 + \epsilon^2)\left(W_x \circ \circ G_{\epsilon/\sqrt{2}}\right)(\sqrt{1 + \epsilon^2}q, \sqrt{1 + \epsilon^2}p). \tag{1.5.28}$$

If we now define $\eta = 1/(1 + \epsilon^2)$, we obtain

$$W_{U'}(q,p) = \frac{1}{\eta} \left(W_x \circ \circ G_\lambda \right) (q/\sqrt{\eta}, p/\sqrt{\eta}), \tag{1.5.29}$$

with $\lambda = \sqrt{(1-\eta)/2\eta}$. This results is exactly similar to the beam-splitter model of linear losses in Eq.(1.3.47) of Sec.1.3.4. In the case that U is normalized at the raw shotnoise standard deviation of X_0, according to results 3) we can achieve the tomography reconstruction of the Wigner function W defined by

$$W(q,p) = \left(W_X \circ \circ G_\sigma \right) (q,p). \tag{1.5.30}$$

This formula is exactly the outcome of unity gain teleportation (see Chap.**??** for details). In both cases, the electronic noise from the homodyne circuit adds a Gaussian filtering process to the reconstructed Wigner function and decreases the quality of the tomographic reconstruction. Although this analysis appears to be unnecessary and somewhat redundant with the results of Eqs.(1.5.14) and (1.5.17), it can easily be applied to broadband photocurrent operators and random variables of Eqs.(1.5.8) and (1.5.12) in the multimode regime. As is shown in Chap.**??**, this property is crucial to understand practical experimental handling of a noisy broadband photocurrent where, for example, the effect of electrical high pass filter needs to be accounted for precisely.

1.5.4 Avalanche regime

A photodiode operated in the avalanche regime is simply reverse biased with a much stronger voltage. In this regime, the voltage bias is large enough so that the internal gain inside the semiconductor triggers an avalanche of charge carriers for every photoelectric conversion event. In practice the avalanche is amplified to be large enough for a visible current spike to appear and to be detected by some external circuitry. After the current spike detection, the external circuit pulls off immediately the reverse voltage bias and waits for the avalanche carriers to dissipate. Once the diode is quiet enough and ready for the next avalanche, the external circuit rearms the reverse voltage bias. This trigger pulling and rearming mechanism induce a recovery time where the photodiode is blind to incoming light. This recovery time also puts a maximum to the rate of detections per second.

In the avalanche regime, the photodiode acts as a Geiger counter able to detect individual photons at precise time. This behavior is crucial for the generation of non-classical non-Gaussian states of light as explained in Chap.**??**. At the quantum level, avalanche photodiodes are effectively sensible to single quanta of light. They can be used to detect single photons and therefore are the perfect non-linear detector for many experiments in quantum optics, both in the qubit and continuous variable regimes. There are several ways to model the measurement operator describing the action of the avalanche photodiode, all of them being equivalent in the case of a very weak incoming light flux.

Click detector

The click detector model assumes that the action of the avalanche photodiode is equivalent to $\hat{a}$. The measurement is written

$$\hat{\rho} \to \hat{\rho}' = \hat{a}\hat{\rho}\hat{a}^\dagger / \mathrm{tr}\left[\hat{a}\hat{\rho}\hat{a}^\dagger \right]. \tag{1.5.31}$$

Since the photodiode absorbs the light, the degrees of liberty of the incoming mode of light are traced out, and the formulation of Eq.(1.5.31) is only relevant if $\hat{\rho}$ is a multimode density matrix. More precisely, Eq.(1.5.31) should therefore reads

$$\hat{\rho}_{1,2} \to \hat{\rho}'_1 = \mathrm{tr}_2 \left(\hat{a}_2 \hat{\rho}_{1,2} \hat{a}_2^\dagger \right) / \mathrm{tr}_{1,2} \left(\hat{a}_2 \hat{\rho}_{1,2} \hat{a}_2^\dagger \right). \tag{1.5.32}$$

There are different consequences to Eqs.(1.5.31) and (1.5.32) that are illustrated in Sec.**??**. With the correspondence rules of Eqs.(1.3.20), we find on the 2-modes Wigner function $W_{1,2}(q,p,q',p')$

$$W_2'(q,p) \propto \int \int dq'dp' \left((q' + \partial_{q'})^2 + (p' + \partial_{p'})^2 \right) W_{1,2}(q,p,q',p'), \qquad (1.5.33)$$

where (q',p') is the mode measured by the photodiode. This is the most simple model to describe an avalanche photodiode and it hides many operational details, yet it is surprisingly efficient to understand the physics of photon subtracted states. The click detector model works especially well when photon number states higher than $|1\rangle$ incoming at the photodiode are rare events.

On/Off detector

Although an avalanche photodiode cannot discriminate between a one photon avalanche or a two photons avalanche, it is necessary to include the detection events beyond $|1\rangle$. The on/off detector models assume that the avalanche photodiode can trigger an avalanche on any quantum states which is not the vacuum state. The measurement operator model is thus a 2 operators POVM model, with $\hat{\Pi}_{\text{off}}$ describing no incoming light

$$\hat{\Pi}_{\text{off}} = |0\rangle\langle 0|, \qquad (1.5.34)$$

and $\hat{\Pi}_{\text{on}}$ describing any incoming light

$$\hat{\Pi}_{\text{on}} = \sum_{n \geq 1} |n\rangle\langle n| = \hat{\mathbb{1}} - \hat{\Pi}_{\text{off}}. \qquad (1.5.35)$$

This model easily translates in the Wigner function formalism into

$$W'(q,p) = 2\pi \int \int dq'dp' W_{\text{det}}(q',p')W(q,p,q',p'), \qquad (1.5.36)$$

where W is the incoming 2-modes Wigner function and W_{det} is the Wigner operator of $\hat{\Pi}_{\text{on}}$ given by

$$W_{\text{det}}(q,p) = \frac{1}{\pi} \left(\frac{1}{2} - e^{-q^2-p^2} \right). \qquad (1.5.37)$$

There are significant differences between the click detector and on/off detector models only when higher photon number events are common enough. However, in this regime, the quantum efficiency of the photodiode becomes more and more important for the precise accounting of photon number events detection probabilities.

Number resolving detector

The photon number resolving detector is an ideal model far from the reality of the avalanche photodiode. It is however interesting to consider it for the theory of photon subtraction. The photon number detector is described by the set $\{\hat{\Pi}_n\}$ of projectors onto number states

$$\hat{\Pi}_n = |n\rangle\langle n|. \qquad (1.5.38)$$

By combining the on/off detector model of Eq.(1.5.35) with the photon number projectors of Eq.(1.5.38), it is possible to develop a POVM model which describes very well physical avalanche photodiode detectors[43].